Diffraction dissociation: 35 years on

N. P. Zotov and V. A. Tsarev

Institute of Nuclear Physics, Moscow State University

P. N. Lebedev Physics Institute, Academy of Sciences of the USSR

Usp. Fiz. Nauk **154**, 207–242 (February 1988)

A review is given of the history of one of the most interesting phenomena in high-energy physics, namely, diffraction dissociation (DD) of hadrons. It was predicted more than 50 years ago by Pomeranchuk and Feĭnberg and has for many years occupied an important place in experimental high-energy studies on major accelerators across the world. This review presents a reasonably complete account of the main experimental results and of the more "settled" theoretical models of DD. Although the discussion is mostly restricted to single nucleon DD, it nevertheless provides a basis for a relatively complete description of this phenomenon. The historical approach adopted in this review to experimental studies of DD is emphasized by numerous references to pioneering work. The last part of the review is devoted to the leading experimental results on DD, obtained during the last five years and not covered by previously published reviews. The new experimental data reveal sufficiently clear evidence for the parton structure of the excited system and of the pomeron. It is emphasized that an understanding of the DD mechanism is crucial to the solution of the confinement problem in the theory of strong interactions, and requires further experimental and theoretical investigation.

TABLE OF CONTENTS

INTRODUCTION

In 1953, I.Ya.Pomeranchuk and E. L. Feĭnberg published a paper entitled "On external (diffraction) generation of particles in nuclear collisions."[1] In this short paper, consisting of only three pages, they predicted a new type of process, namely, inelastic diffraction scattering, or diffraction dissociation (DD), and discussed the leading features of these processes. In particular, they noted that inelastic diffraction scattering can occur in all cases in which the "coherence" condition $q_{\parallel} R \ll 1$ is satisfied ($q_{\parallel}$ is the longitudinal component of transferred momentum q). This condition ensures that the target participates in the process as one whole, and absorption that is responsible for it occurs on the periphery, i.e., in a *skin layer* of thickness $d \ll q^{-1}$. In the thirty-odd years since then, the study of this very interesting phenomenon has occupied an important place in research programs on major accelerators across the world, and the phenomenon itself has been the subject of numerous theoretical investigations.

Diffraction phenomena are well-known in classical physics where they are determined by interference between waves scattered by different objects. In elementary-particle physics, the analog of these phenomena is elastic diffraction scattering of quantum-mechanical waves describing high-energy hadrons. Inelastic processes are the physical cause of this scattering. Numerous new particles can be created in collisions between high-energy hadrons. These inelastic channels are responsible for partial absorption and the associated change in the wave function of the initial hadron in the region in which the interaction takes place. The linear size R of this region is of the order of the range of the strong interaction, i.e., of the order of the size of hadrons (~ 1 fm). This is, in fact, the "black" or "grey" disk that produces the characteristic diffraction pattern on a "screen," i.e., in a recording instrument. The geometric and kinematic conditions corresponding to the scattering of high-energy hadrons are analogous to the conditions under which diffraction phenomena are usually considered in optics. Actually, at incident-hadron energies in excess of a few GeV, the wavelength of the hadron is much smaller than the characteristic (lateral) size R of the target, so that the well-known condition of diffraction theory, i.e., "short wavelength," or $kR \gg 1$, is satisfied where $k = 2\pi/\lambda = p/\hbar \simeq 5 \cdot 10^{13}\, p(\text{GeV}/c)^{-1}\ \text{cm}^{-1}$ is the wave vector of the incident hadron, $p = (E^2 - m^2c^4)^{1/2}c$ is the momentum of the hadron, and E, m are, respectively, the energy and mass of the hadron. We also know that the other condition ("long distances") is also satisfied, i.e., $R/D < 10^{-13} \ll 1$, since for real instruments the distance D between the target and "screen" (detector) is macroscopic. Finally, even at the highest energies that are at present available to experimenters in cosmic rays, we have $kR < 10^8$, so

 0038-5670/88/020119-21$01.80

that $kR_T^2 D^{-1} < 10^{-5} \ll 1$, i.e., the diffraction scattering of hadrons by nucleons and nuclei corresponds to classical Fraunhoffer diffraction. When the paper by Pomeranchuk and Feĭnberg was published, this analogy between elastic scattering of hadrons and classical diffraction was already well understood and was used to describe the scattering of nucleons and pions by nucleons and nuclei. The fundamentally new step taken by Pomeranchuk and Feinberg in passing from classical fields to fields describing relativistic particles was to take into account the quantum-field character of the interacting objects. It is indeed the presence of internal degrees of freedom in the interacting hadrons, which can be excited in the scattering process, that is the reason for the special diffraction phenomena that arise when microparticles are scattered. They have no analogs in the diffraction of classical waves.

While emphasizing this fundamental novelty of the diffraction dissociation of hadrons, we note the heuristic role that the theory of electromagnetic radiation has played in this context, as is perfectly clear from the paper by Pomeranchuk and Feĭnberg. They argued that diffractive creation of hadrons was unavoidable and wrote "it is usually considered that this effect (i.e., the appearance of the diffracted wave as a result of absorption—N. Z. and V. Ts.) manifests itself only as elastic scattering. However, the change in the motion of a charge that is produced as a result of this scattering gives rise to the emission of gamma rays (for example, when pions are absorbed by nuclei). It is clear that such diffraction scattering of nuclear-active particles (nucleons, pions) must be accompanied by the emission of pions and, possibly, nucleon pairs as well."[1]

The phenomenon of diffractive production of hadrons can be explained in terms of a model borrowed from classical wave scattering by assigning "internal degrees of freedom" to the classical wave. Polarization can play the part of these degrees of freedom.

For example, consider the scattering of light by an object ("screen") that has different refractive indices for right and left circularly polarized rays.[2,3] Suppose further that the incident light is linearly polarized. Since the scattering matrix in the basis of the linearly polarized states is nondiagonal, diffraction scattering should result in two different waves, one of which has the same polarization as the initial wave and the other a perpendicular polarization. The latter was not present in the incident wave and therefore may be looked upon as a result of "diffractive production."

The prediction of Pomeranchuk and Feĭnberg was brilliantly confirmed by experimental studies performed in the subsequent years. In the mid 1960s, after the advent of high-energy accelerators, diffraction dissociation was discovered in experiments with proton and pion beams. Subsequent studies showed that the diffraction mechanism for the generation of particles is one of the leading processes contributing to the total cross section for hadron interactions at high energies. Intensive experimental and theoretical studies have provided much information on the properties of diffraction dissociation, and have thrown light on the internal structure and the interaction of hadrons. The result has been a deeper understanding of the nature of the "internal degrees of freedom," or virtual states, whose fluctuations are responsible for the high probability of inelastic diffraction observed experimentally. Initially, the eigenstates of the diffraction scattering matrix were identified with states containing a certain number of virtual pions close to the mass surface. Elastic diffraction scattering of these pions, which constitute the "cloak" of the nucleon, and the transfer of some momentum to them, violated the coherence of the initial system and translated the scattered pion into a real state. This approach was embodied in the Drell-Hiida-Deck model[4] which is widely used in the description of diffraction dissociation to states with low mass of the final system. This model has been continually refined and is capable of reasonably successful description of many of the properties of inclusive and exclusive diffraction dissociation cross sections found in experiments with nucleon, pion, and kaon beams.

There has also been another tendency that, in some sense, has taken the opposite route, i.e., the structures found in the region of low masses of the created system were interpreted as resonance states of initial hadrons.

However, detailed comparisons between the predictions of the two models with experiments on diffraction dissociation and with the data produced by partial-wave analysis of the amplitudes of binary processes has shown that neither of them is capable of describing *all* the features of the phenomenon and that, probably, the most adequate model must take into account both mechanisms and must contain resonance and nonresonance contributions (this is the so-called "two-component" model). Detailed partial-wave analyses of the excited system produced as a result of the diffraction process have played an important role in the elucidation of the peaks in the diffraction dissociation spectrum.

At first, there was a widely held view that diffraction dissociation was specific only to the excitation of hadrons to low-mass states. It was not until 1973, i.e., twenty years after the prediction of Pomeranchuk and Feĭnberg, that colliding-beam experiments performed at CERN resulted in the discovery of the diffractive excitation of nucleons to high-mass states.[5] The phenomenon was subsequently investigated in great detail in collaborative Soviet-American experiments on the accelerator at Batavia[6–8] and in a number of other experiments. The results of these experiments attracted considerable attention and produced a flood of theoretical papers concerned mostly with phenomenology, based on the Regge field theory and on analyses performed within the framework of the impact parameter representation. In this approach, data obtained at high energies could be much more reliably and specifically used (than was done at low energies) to separate out and analyze the contribution of the diffraction mechanism and to gain a better understanding of its role in high-energy hadron interactions.

Subsequent advances in the theory of diffraction phenomena were due to the development of the quark-parton picture of hadron structure and of quantum chromodynamics, which have given a whole new meaning to the concept of internal degrees of freedom of hadrons, and have produced a new language for the interpretation of diffraction phenomena. This, in turn, naturally gave rise to the examination of the two components of diffraction dissociation in the low-mass region on a unified basis, i.e., in terms of the model of component quarks. The quark-parton idea has also turned out to be fruitful in relation to diffractive excitation in the high-mass region. Here, the combination of the achievements of the Regge model and the elements of quantum

chromodynamics has led to phenomenological schemes that successfully describe many of the features of diffractive hadronic processes.

During the past thirty years, diffraction dissociation has attracted many hundreds of original theoretical and experimental papers and a number of reviews[3,9–25] that provide a detailed discussion of the different aspects of diffraction phenomena. The present review lays no claim to completeness. On the contrary, it is a brief survey of experimental and theoretical studies of diffraction dissociation. Its aim is to exhibit the physical richness of this phenomenon, which promises to be an interesting area of research both on existing accelerators and on accelerators of the next generation. In order not to lose our way in the maze of experimental data and different theoretical models, we have deliberately reduced our field of view and have confined our attention mostly to the single nucleon diffraction dissociation. This means that we shall ignore interesting questions such as double diffraction dissociation and double pomeron exchange, diffraction by nuclear targets, diffractive production of heavy quarks, and a number of other questions. Important data on the diffraction dissociation of pions and kaons will be touched upon only briefly. Moreover, we shall concentrate on features that are specific to inelastic diffraction and distinguish it from elastic diffraction scattering. These are questions that relate to the excitation of the internal degrees of freedom of the hadron. In addition, we shall be forced to ignore almost entirely the important problem of the pomeron common to elastic and inelastic diffraction, the exchange of which leads to diffraction phenomena. At the same time, we shall be acutely aware of the clear artificiality of the separation of the question "how is the hadron excited?" from the question "what is it excited by?" Nevertheless, we shall use this subdivision since the pomeron problem is discussed in detail in a number of reviews.[12,20,21,23,25–27] Section 2 of this review is devoted to the consideration of the principal features of experimental data on inclusive and exclusive cross sections for diffractive excitation to low-mass states, and to the discussion of these data in terms of different theoretical approaches. In Section 3, the same program is applied to the high-mass region. Section 4 deals with new results, obtained in the last few years, which have resulted in further advances in our understanding of the nature of diffraction dissociation.

2. DIFFRACTION DISSOCIATION TO LOW-MASS STATES

2.1. Experimental results

The first experimental results on the diffraction dissociation of hadrons were concerned with the near threshold excitation of nucleons in experiments commonly known as the "missing-mass method."[28–31] In this technique, the momentum of the scattered hadron is measured and the mass M_X of the excited system is then determined from the laws of conservation of energy and momentum.

Figure 1a shows a typical missing-mass spectrum for the diffractive excitation of protons by negative pions $\pi^- p \to \pi^- X$ for incident-pion momenta of 8 GeV/c, as reported[1)] in one of the first experiments on diffraction scattering.[30] As can be seen, there are well-defined peaks at $M_X \simeq 1.4$ and $M_X \simeq 1.7$ GeV. Similar peaks were found somewhat later in pion and kaon mass spectra. The questions are: what is the nature of these peaks and do they represent the resonance excitation of the incident hadrons? These questions have been the subject of a lively discussion for many years, and continue to be discussed to this day. We shall examine this problem somewhat later; for the moment, we note that even the very early experiments indicated that the peak on the $d\sigma/dM_X$ curve near the mass threshold and the peaks at the higher masses were probably of different origin. The first thing to note is that they have different widths. While the peak at $M_X \simeq 1.7$ GeV has the normal width $\Gamma \simeq 100$ MeV, typical for nucleon resonances, the near-threshold peak at $M_X \simeq 1.4$ GeV is significantly broader. The other difference is due to the different dependence of the cross section on the transferred momentum $|t|$. This can be seen from Fig. 1b which illustrates the excitation of a proton in the process[32] $pp \to pX$. As $|t|$ increases, the first peak rapidly flattens out whereas the second becomes better defined.

The main disadvantage of the missing-mass method is the absence of any information about the decay properties of the created system. This information was obtained in experiments with bubble chambers and spark spectrometers, which are widely used in studies of diffraction dissociation into exclusive channels in colliding beams of ISR at CERN and also on the FNAL and IFVE accelerators. Diffractive excitation of the proton to the system $(n\pi^+)$ for $s^{1/2} = 45$ GeV was investigated in this way.[33] Figure 2 shows the mass

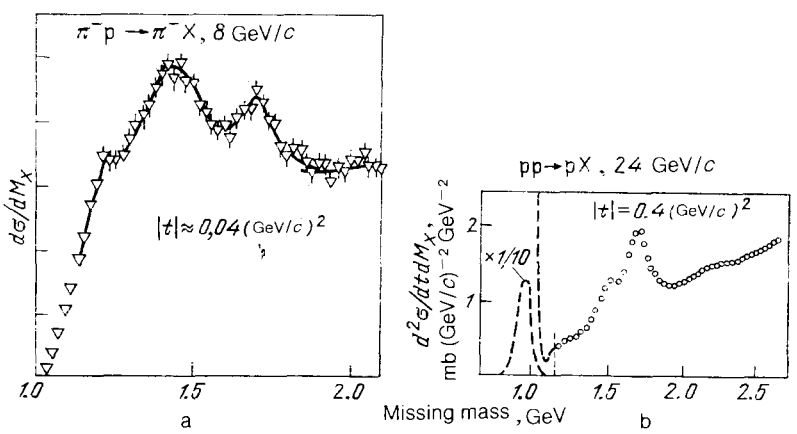

FIG. 1. Missing-mass spectrum for proton DD in the process $\pi^- p \to \pi^- X$ (experimental data taken from Ref. 30) (a) and in the process $pp \to pX$ (experimental data taken from Ref. 32). (b) Broken lines show the elastic pp scattering peak.

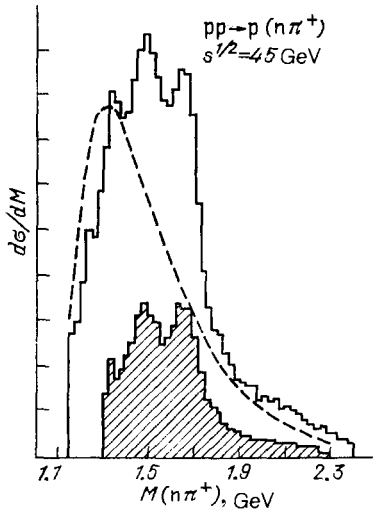

FIG. 2. Mass distribution of the $(n\pi^+)$ system in the $pp \to p(np^+)$ process.[33] Broken line—theoretical calculations based on the DHD model.[3]

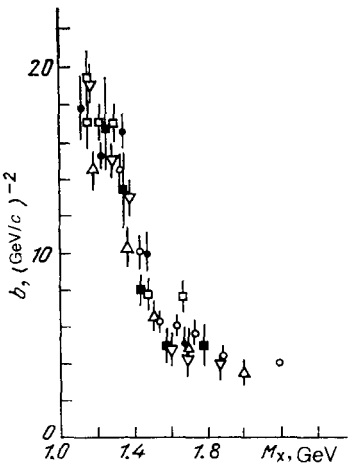

FIG. 3. Slope parameter as a function of the mass of the excited system in proton DD at energies between 19 and 1500 GeV. A compilation of experimental data can be found in Ref. 39.

distribution of the $(n\pi^+)$ system, which again clearly shows the presence of the same peaks. Signals due to the excitation of these states are enhanced relative to the background for a particular restriction on the momentum transferred from the proton to the neutron (shaded area in Fig. 2).

These investigations of the exclusive processes $NN \to (\pi N)N$, $NN \to (\pi\pi N)N$, $\pi N \to \pi(\pi N)$, $\pi N \to (3\pi)N$, $KN \to (K\pi\pi)N$, and also the inclusive experiments on diffraction dissociation, have revealed[33-39] the presence of many features showing a similarity between inelastic and elastic diffraction. Thus, first, there is the weak dependence on energy, which is typical of diffraction phenomena. The cross sections for diffractive generation flatten out at FNAL energies (~ 300 GeV) and gradually increase at ISR energies. For example, the DD cross section for the process $np \to (p\pi^-)p$ with masses of the excited system in the range $1 < M_X < 1.45$ GeV are almost constant between 100 and 300 GeV (Refs. 33, 35, and 36), and the cross section for the process $pp \to p(p\pi + \pi^-)$ at ISR energies increases very slowly.[34]

As for elastic processes, the differential DD cross sections have well-defined peaks corresponding to forward scattering, which can be described by the exponential expression $d\sigma/dt = (d\sigma/dt)_0 e^{bt}$, where the slope parameter for elastic scattering is $b \simeq 8$–12 $(\text{GeV}/c)^{-2}$, depending on the particular process and the range of values of s and t. The slope parameter b depends not only on the particular type of DD process, but is also very dependent on the mass of the excited system. It is much greater near the excitation threshold than for elastic scattering, and thereafter decreases rapidly with increasing mass. Figure 3 is a compilation[21] of experimental data on the slope parameter b for exclusive nucleon diffraction dissociation.[39] It is clear that, for low masses of the excited system, the slope parameter is greater by a factor of almost two than for elastic pp scattering, whereas for $M_X \sim 1.6$ GeV it is lower by a factor of two than for elastic scattering. This correlation between the slope parameter and the mass of the excited system is a common property of diffraction dissociation processes in the low-mass region.

As for elastic scattering, the diffraction peak becomes narrower in diffraction dissociation as the energy increases. For example, the slope parameter for the $pp \to p(\pi^+ n)$ process in the range $24\ \text{GeV}/c < p < 1500\ \text{GeV}/c$ increases with increasing s at roughly the same rate as in elastic scattering.

The common feature, typical of differential cross sections for the elastic diffraction scattering of hadrons by nucleons, is also the presence of structures resembling diffraction minima. In pp scattering, there is a minimum at $|t| \sim 1.1$–1.4 $(\text{GeV}/c)^2$ whereas in πp scattering this occurs at $|t| \sim 4$ $(\text{GeV}/c)^2$. An analogous structure has also been seen in the DD cross section for the process $pp \to (n\pi^+)p$ (Ref. 33; Fig. 4), but in contrast to elastic scattering this is found to lie at the significantly lower values $|t| \sim 0.2$–0.3 $(\text{GeV}/c)^2$, as expected.[40]

Measurements of the angular distribution of the decay products of the excited system are important for an understanding of the mechanisms responsible for diffractive generation. Several experiments on nucleon DD have revealed "forward peaks" in the distribution over the Gottfried-Jackson angle, i.e., for $\cos\theta \simeq 1$, indicating the preferential emission of a nucleon by the excited system in the direction of the incident-nucleon momentum. Moreover, relatively unex-

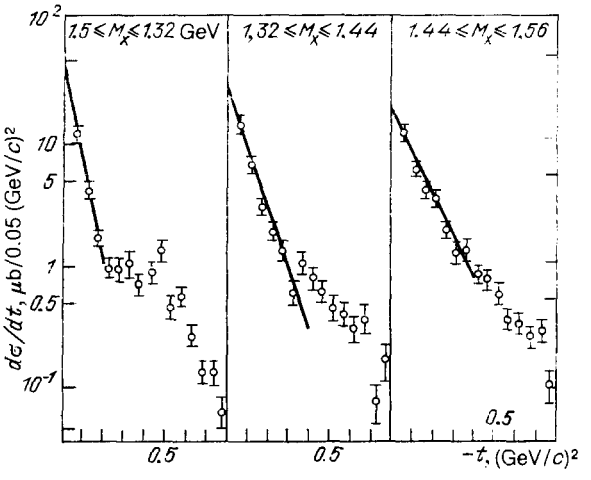

FIG. 4. Differential cross sections for the $pp \to p(np^+)$ process with $s^{1/2} = 53$ GeV (Ref. 53).

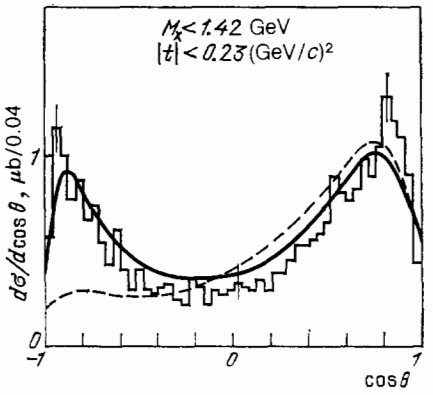

FIG. 5. Distribution over the cosine of the Gottfried-Jackson angle for the $np \to p\pi^-(p)$ process with $p_L = 60$ GeV/c (Ref. 39). The theoretical curves are the predictions of the DHD model with allowance for π and N exchange (solid curve) and π exchange alone (broken curve).

pected and, from the theoretical point of view, very critical discovery was that of the presence of the backward peak ($\cos\theta \simeq -1$), revealed by detailed studies of neutron DD to the system ($p\pi^-$) (Fig. 5) on the IFVE accelerator[14,39] in the energy range 35–65 GeV.

So far, we have been discussing nucleon DD. The mass spectra obtained for pion and kaon DD into the 3π and $K\pi\pi$ states, respectively, exhibit the same characteristic features.[37,38] They rapidly increase at the threshold, reach a maximum for M_X of about 250 MeV above the threshold, and then rapidly decrease for $M_X > 1.5$ GeV. Thus, the 3π excitation spectrum is characterized by a wide maximum in the range $1 < M(3\pi) < 1.4$ GeV, with superimposed peaks due to the creation of the so-called A_1, A_2, and A_3 states. Peaks corresponding to the Q(1300), K*(1420), and L(1770) states can be seen in the spectrum of the ($K\pi\pi$) system.

An important stage in the study of DD was the detailed partial-wave analysis of the diffractively excited 3π system.[37] This showed that the phases of the partial amplitudes that predominate in A_1 (for $M \simeq 1.1$ GeV) and A_3 peaks do not show a resonance behavior. An unambiguous conclusion about the resonance behavior of the phase in the Q-enhancement region in the mass spectrum of the $K\pi\pi$ system cannot be made either.

This concludes our brief presentation of the main experimental facts relating to DD to low-mass states. Additional information on the finer details of experimental data will be touched upon in the next Section when we discuss theoretical models of DD.

2.2. Diffraction eigenstates, the Drell-Hilda-Deck model, and quarks and gluons

The interesting properties of DD processes, discovered as a result of inclusive and exclusive experiments, have fueled theoretical studies aiming at a detailed quantitative picture of inelastic diffraction scattering.

The generalized formalism for the description of inelastic diffraction, which developed the idea of the quantum-field nature of the DD, was given by Good and Walker.[2] In this approach, the initial state of the hadron, and any physical state to which it can undergo a diffractive transition, is represented by a superposition of "bare" states that are the

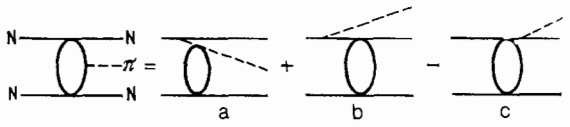

FIG. 6. Diagrams for the dissociation process $NN \to (pN)N$.

eigenstates of diffraction scattering:

$$|h_i\rangle = \sum_k U_{ik} |\chi_k\rangle. \tag{2.1}$$

Each of these bare states is absorbed by the target in a different way (adsorption into nondiffractive channels), leading to different mixing of these states in the final state. The amplitude for the diffraction transition between two physical states has the form

$$\langle h_i | T | h_j\rangle = (1-\eta_i)\,\delta_{ij} - \sum_k (\eta_k - \eta_i)\, U_{jk} U^{-1}_{ki}, \tag{2.2}$$

where η_k are the absorption parameters of the bare states. It is clear from this that inelastic diffraction occurs only if $\eta_k \neq \eta_i$ for at least some values of k, i.e., if absorption changes the relative weights of the states $|\chi_k\rangle$ in the initial superposition (2.1).

One of the most successful implications of this general idea is the Drell-Hiida-Deck model (DHD)[4] for the description of near-threshold low-mass excitations in which virtual states are close to real physical states of particles, i.e., the matrix elements are

$$U_{ij} = \delta_{ij} + \varepsilon_{ij}, \quad \varepsilon_{ij} \ll 1. \tag{2.3}$$

For example, for the DD process $N \to \pi N$, it follows from this that simple diagrams describing this process (Fig. 6) include the decay $N \to \pi N$ and the elastic diffraction scattering of the π and N by the target. Calculations show that the contributions of diagrams b and c of Fig. 6 are comparable in magnitude but have opposite signs. This means that a considerable degree of cancelation of these contributions occurs in the region of the kinematic variables in which $|t|$ and M_X are small, and the total amplitude for the process $NN \to \pi NN$ is described with good precision by the single amplitude corresponding to the Drell-Hiida-Deck diagram[4] (Fig. 6a). This diagram is shown in Fig. 7a with the relevant annotation.

Since, by hypothesis, the bare particles are close to real particles, the amplitude that corresponds to this diagram does not contain unknown parameters and predicts the DD behavior in terms of directly measurable quantities, namely,

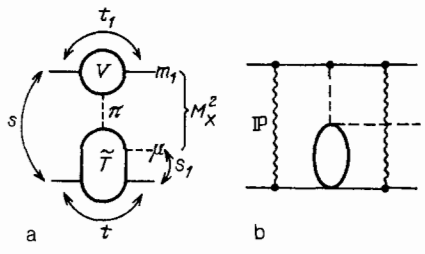

FIG. 7. DHD diagram for the process $NN \to (pN)N$. a—π exchange, b—π exchange with absorption.

the πNN coupling constant and the amplitude for the elastic scattering of the real pion by the nucleon. However, this naive model is in poor agreement with experiment, since it predicts higher cross sections, wider mass distributions, and smaller angles of the diffraction cone. A reasonable description of the experimental data by the low-mass DD process can be achieved only by introducing an additional dependence on the transferred momentum at the πNN vertex which is usually interpreted in terms of the departure of the pion from the mass surface. The DHD model is widely used in this form to describe diffraction dissociation (see, for example, Refs. 13, 14, 16, and 41), and successfully explains many of the characteristic features of DD, including the following:

1) weak energy dependence, which is the result of the weak energy dependence of the πN scattering cross section;
2) predominance of vacuum exchange;
3) approximate equality of the DD cross sections for particles and antiparticles;
4) factorization property;
5) predominance of the $\pi + X_1$ decay.

Some of the properties of DD arise in this model as a consequence of kinematics.

1. The peaks at low masses are of kinematic origin and are due to two factors, namely, the phase factor which ensures that the amplitude vanishes at the threshold $M_X = m_1 + \mu$, and the fall in the matrix element for large M_X due to the peripheral effect.

2. The strong dependence of the slope parameter in the differential cross section $d\sigma/dt$ on the mass M_X can be explained as a consequence of the double peripherality of the DHD diagram (see Fig. 7a): $T \sim \exp(bt + b_1 t_1)$. At the threshold, $M_X = m_1 + \mu$ and t_1 and t are linearly related, so that $T \sim \exp[(b + b_1)t]$. As M_X increases, the dependence of t_1 on t becomes weaker, and this leads to a weaker dependence of the amplitude T on t.[3)]

3. The difference between the positions of the peaks corresponding to the πN and $\pi\pi$N channels of DD is naturally explained by the difference between the masses of the final states.

However, the strong dependence of the slope parameter on the mass of the excited system was a stumbling block for the DHD pion exchange model. Detailed analysis of the behavior of the cross section for the process $pp \to pn\pi^+$ as a function of all four kinematic variables has shown that kinematics alone is not sufficient to reproduce the entire dependence of the slope parameter b on M_X, and experimental data indicate that an additional M_X dependence of the parameter b should be explicitly present in the matrix element. Another characteristic feature of the differential DD cross section in the low-mass region is, as already noted, the structure at $|t| \simeq 0.2$–0.3 $(\mathrm{GeV}/c)^2$, which is an argument in favor of the peripheral character of the DD process (i.e., the profile of the amplitude for this process in the impact parameter representation should have a maximum at a distance of the order of the nucleon radius), whereas the profile of the DHD pion-exchange amplitude, which gives a smooth t dependence for the differential cross section, is a Gaussian and resembles the profile function for elastic scattering.[16] Tsarev[40] (see also Ref. 43) has indicated a way of resolving these difficulties: absorption effects due to the redistribution of particles in the initial and final states must be taken into account Fig. 7b. Absorptive effects lead to a significant modification of the scattering amplitude.[15,16,40]

1. The absolute magnitude of the DD cross section decreases by approximately a factor of two as compared with the prediction of the DHD pion-exchange model (without form factors).

2. Additional t and t_1 dependences appear, which means that there is no need to introduce large non-mass corrections.

3. The slope parameter in the differential cross section increases in the region of low masses M_X, and there is an enhanced correlation between b and M_X. The resultant correlation between the slope parameter and the mass is a superposition of kinematic and dynamic correlations.

4. Absorption leads to the suppression of central contributions and gives a peripheral profile for the DD amplitude in the impact parameter representation. This is responsible for the differential cross section minimum for small M_X at $|t| \simeq 0.2$–0.3 $(\mathrm{GeV}/c)^2$, which is confirmed by experimental data obtained at CERN and at Batavia.[33,35,36]

Because of the considerable cancelation of crossover diagrams in the region of small $|t|$ and M_X, we have neglected the contributions due to them. It was noted in Refs. 41 and 44 that experiments suggest that these diagrams play a significant role in a certain range of values of the variables. One argument relies on the phenomenon of "crossover" in the reactions $K^0(\bar{K}^0)p \to Q^0(\bar{Q}^0)p$ and $\pi^\pm p \to \pi^\pm (\pi^- \Delta^{++})$ which can be simply explained in terms of K^* and Δ exchange when the crossover diagrams are taken into account. The other argument is based on correlations between the decay products of the excited system in the $np \to (\pi^- p)p$ reaction in the polar and azimuthal angles,[35,36] which cannot be explained by the DHD pion-exchange diagram alone. It would seem that the experimental peak at $\cos\theta = -1$ and $\phi = 0$ can be explained by taking into account nucleon exchange[12,35,41] (Fig. 6b). However, the predictions of this model in relation to the ϕ-distribution become significantly different when nucleon spin is taken into account in the DHD diagrams. In this respect, the most rigorous approach is that in which all three DHD diagrams (see Fig. 6) are taken into account, including the spins of the nucleons and the π-exchange diagram with absorption.[14,39] The point is that when the model described in Ref. 40 is used as a basis for the absorption corrections to all three diagrams of Fig. 6, the absorption corrections to the crossover graphs cancel out, and the DD amplitude can be represented by the DHD π-meson contribution with absorption and crossover contributions without absorption.

In the foregoing discussion, the bare states included only states close to real particles. It is natural to suppose that the spectrum of bare states is wider, and includes the resonances. As we have seen, the contribution of the latter is quite clear in the DD mass spectrum. Apart from the creation of resonances through the DHD mechanism (diffractive excitation $N \to \pi\Delta \to \pi\pi N$), we can also have direct creation which can be represented by Figs. 8a–c.

The "two-component" model that includes the contribution of the DHD amplitude and the direct creation of resonances was first put forward in Ref. 45 for the description of ρ-meson photoproduction, and has seen been widely used.[4)] The presence of the resonance contribution to DD

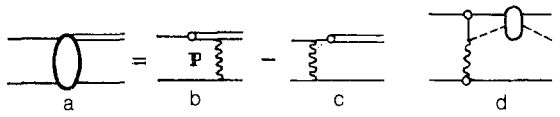

FIG. 8. Direct creation of resonances in DD processes (a–c) and pion creation via the DHD mechanism with rescattering (d).

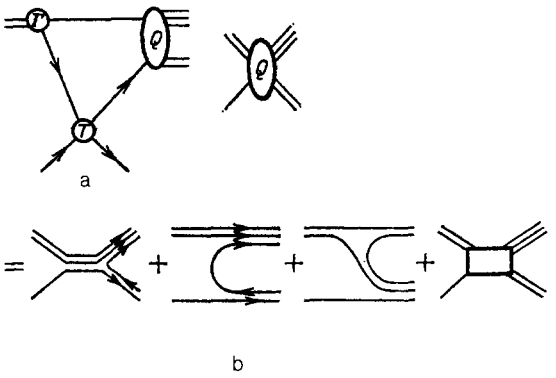

FIG. 9. DD diagrams for the process $N \to \pi N$ in the quark model.[46]

can be reconciled in the two-component model with the nonresonance behavior of the phase of the corresponding partial wave, which is very important in view of the above nonresonance behavior of the phases for many of the pion and kaon peaks in DD. This is so because unitarity demands that the contributions of DHD and of direct resonance creation must be taken into account at the same time as the resonance rescattering of particles created by the DHD mechanism (Fig. 8d). If this is so, then, under certain relatively natural assumptions about the phase of the DHD amplitude, we find that the resonance behavior of the phase in the resultant amplitude may be "compensated."

In the "two-component" model discussed above, the contributions of the resonance and nonresonance excitations are completely independent. However, it is natural to suppose that they have a common origin because they relate to the excitation of the same original hadronic system. Attempts to examine the two DD components on a unified basis were made in Ref. 46 (see also Ref. 47) in which the "bare" states were identified with quasifree "dressed" (component) quarks.[48]

The dressed component quarks (or "valons"[49]) provide us with a simple method[50] of reconciling the additive quark model[5] with the quark-gluon picture.[51] The assumption is that the valence quarks are surrounded by their own clouds of gluons and quark-antiquark pairs, by analogy with ordinary particles in quantum field theory. In other words, partons (valence quarks, gluons, and sea quarks and antiquarks) form "clusters," each of which contains a valence quark. When the radius of a cluster of this kind is less than the radius of the hadron, the clouds surrounding the valence quarks do not overlap, and the interaction between the individual "dressed" quarks occurs independently.[48]

It is assumed in Ref. 46 that the component quarks experience only elastic diffraction scattering in DD processes, which occurs by analogy with elastic scattering of hadrons. This interaction should be significant in DD processes with small $|t|$, in contrast to hard scattering in which the interaction in the final state probably produces a small distortion of quark scattering kinematics. This means that the main contribution to DD is provided not by simple pole graphs, as in the DHD model, but by more complicated diagrams such as those shown in Fig. 9.

A strong "confining" interaction between quarks that otherwise would fly apart leads either to their confinement to an excited resonance system or to capture (direct or with recombination) of quark-antiquark pairs from the sea of quarks, giving the quark analogue of the DHD diagrams. The model thus provides a natural unification of aspects of resonance and "direct" interactions. Although calculations based on this model have not as yet been taken to the stage of a detailed quantitative comparison with experiment, qualitative analysis[46] indicates that the model has the advantages of the two-component model and at the same time correctly reproduces some of the DD properties of diffraction dissociation that are difficult to understand within the framework of the two-component model (DD on nuclei, θ-ϕ correlation). On the other hand, there are difficulties in this model due to the excitation of sufficiently large masses M_X for small $|t|$, which requires either a departure of component quarks from the "mass surface"[51] or their excitation after scattering.[52] Both factors indicate that, for large M_X, nonrelativistic component quarks can no longer act as the "bare" states undergoing only elastic diffractive scattering. Relativistic effects and interactions with the gluon component of the hadron play a significant part in this region. It is possible that further refinement of the quark model of DD will also involve the inclusion of fluctuations in the number and rapidities of active (slow) partons belonging to dressed quarks.[53]

The alternative to the valon model[54] is that the gluons are concentrated in the interior of the hadron in the form of a "glueball" and that the gluon distribution is unrelated to the distribution of quarks (with the exception of the limitations imposed by conservation laws). In nondiffractive interactions with low transferred momenta, gluons from one of the hadrons interact with gluons in another, and the resulting excited state of the gluon field acts as a source of pionization in the central region. Quarks pass through freely and, having picked up gluons, provide the leading particles. A similar point of view can serve as a basis for resurrecting the old idea[9] that the peaks play a special part in DD: the D-resonances of Morrison may be looked upon[55] as the bound states of a set of quarks (bearing the quantum numbers of the initial hadron) and an excited glueball. Just as a quark system is readily excited and undergoes a transition to a state with a higher angular momentum[50] one would expect similar excitations in the case of the glueballs, and such excitations predominate in diffractive processes if they are generated by the interaction of glueballs. Glueball models are undoubtedly interesting from the heuristic point of view. However, in their modern formulation they do not enable us to perform detailed calculations of exclusive channels or to predict the internal properties of created states, the mass spectrum, the correlations, and so on. All this makes their experimental verification rather more difficult.

To conclude this Section, we emphasize once again that, despite considerable experimental and theoretical efforts, the nature of the peaks observed in diffraction dissociation for low values of M_X and, in particular, their resonance

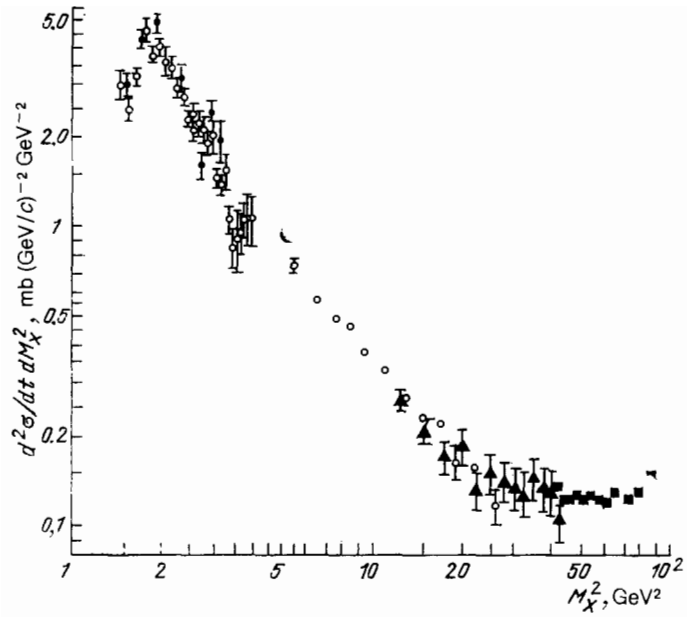

FIG. 10. Differential cross section for the process $pp \to Xp$ as a function of M_X^2 at $s = 500\,\text{GeV}^2$ and $|t| = 0.025\,\text{GeV}/c^2$ (Ref. 15).

character, are often not fully understood. An additional possibility for separating resonance from nonresonance contributions in DD is afforded by studies of the radioactive decay channels of the excited system.[56] The background process (bremsstrahlung) does not then exhibit resonance-like behavior that impedes the identification of true resonances in the case of hadronic final states.

3. DIFFRACTIVE EXCITATION OF STATES WITH HIGH MASS

3.1. Experiments in the high-mass region

Experimental studies of the excitation of protons to high-mass states began, as already noted, with the colliding-beam experiments[5] at CERN. However, the most complete investigation of such processes was carried out in collaborative experiments by Soviet and American Physicists on the FNAL accelerator at Batavia, using a deuterium jet target. The experiments were performed in 1972–1974 and their results have been presented in detail in a review paper.[15]

The experimental data obtained with the deuterium jet target[7,8] resulted in a unification of the then available data from CERN[5] and Batavia[56,57] at high and low masses, and were used to deduce the dependence of the differential cross section[6)] $d^2\sigma/dt\,dM_X^2$ for the process $pp \to Xp$ on M_X^2 (Fig. 10).[6] It is clear that the cross section for fixed $|t|$ and s has a peak in the low-mass region at $M_X^2 \simeq 1.9\,\text{GeV}^2$ and then falls rapidly with increasing M_X^2 in the region up to $M_X^2 \simeq 25\,\text{GeV}^2$. It is important to note that comparisons of pd with pp data were based on the assumption of "nuclear factorization" of pd cross sections:

$$\frac{d^2\sigma}{dt\,dM_X^2}(pd \to Xd) = \left[\frac{d^2\sigma}{dt\,dM_X^2}(pp \to Xp)\right] F_d(p_b, t), \tag{3.1}$$

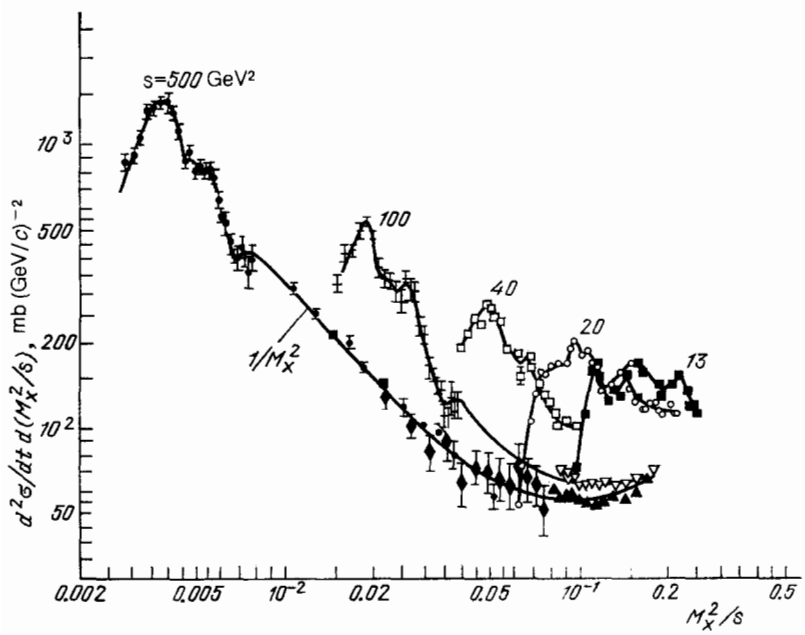

FIG. 11. Differential cross section for the process $pp \to Xp$ as a function of M_X^2/s for $|t| = 0.042$ (GeV/c^2) and different values of s. The compilation of experimental data can be found in Ref. 22.

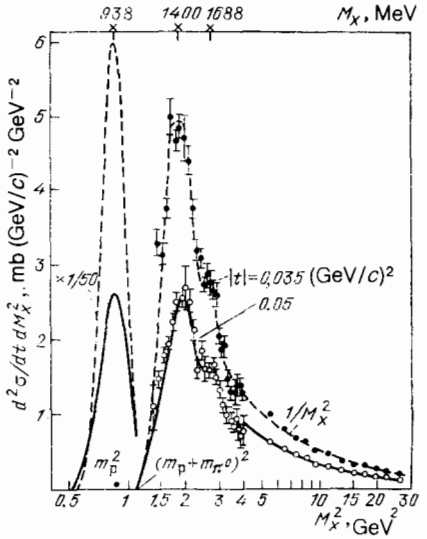

FIG. 12. Differential cross section for the process pp→Xd as a function of M_X^2 for $p_L = 275$ GeV/c and fixed values of $|t|$ (Ref. 8).

where the coherence factor is given by (here and henceforth p_L is the incident-proton momentum in the laboratory frame)

$$F_d(p_L, t) = \left[\frac{\sigma_{tot}^{pd}(p_L)}{\sigma_{tot}^{pp}(p_L)}\right]^2 S^2(t), \tag{3.2}$$

and $S(t)$ is the deuteron form factor. The "dynamics" of the structure of the cross section $d^2\sigma/dt\,d(M_X^2/s)$ for the process pp→Xp can be seen in Fig. 11: as the energy increases, the resonance region shifts toward smaller values of M_X^2/s, whereas high-mass excited states fill the diffraction region and form a smooth continuum.[22]

In the low-mass region ($M_X^2 \lesssim 4$ GeV^2), the experimental data obtained with high resolution for hydrogen[3] and deuterium[7,8] revealed for the first time the high-energy structure and its energy dependence. For fixed $|t|$, the mass spectrum clearly shows a peak in the region of $M_X^2 \simeq 1.9$ GeV^2 and a smaller peak at $M_X^2 \simeq 2.8$ GeV^2 (Fig. 12). Figure 13 compares the structures recorded in the mass spectrum at high and low energies.[30-32] The factorizability of the DD cross sections has been demonstrated by experimental data on pp and pd interactions at high energies[6-8] (Fig. 14).

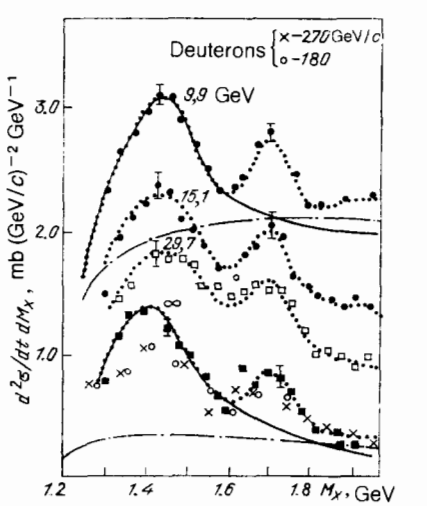

FIG. 13. Mass spectra for the process pp→Xp at high and low energies.[15] Solid and dot-dash curves correspond to the DHD and polynomial-type backgrounds, respectively.

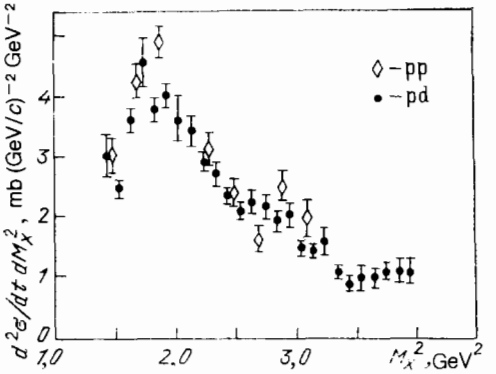

FIG. 14. Comparison of pd cross sections divided by F_d (Ref. 7) with pp data[6] for $p_L = 260$–275 GeV/c.

In the intermediate-mass region ($5 \leqslant M_X^2 \leqslant 0.05s$ GeV^2), the cross sections no longer show a resonance structure and increase rapidly with increasing M_X^2. A numerical fit to the experimental data, based on the formula

$$\left.\frac{d^2\sigma}{dt\,dM_X^2}\right|_{|t|=0,05} = D(s)(M_X^2)^{-\alpha(s)} \tag{3.3}$$

shows that the function $\alpha(s)$ is close to unity and is practically independent of s. The $1/M_X^2$ dependence of the cross section $d^2\sigma/dt\,dM_X^2$ was subsequently confirmed at FNAL on the basis of larger statistics for $0.02 \leqslant |t| \leqslant 0.18$ (GeV/c)^2 and $122 \leqslant s \leqslant 699$ GeV^2, and also by new experimental pp data obtained with the ISR colliding beams for $23.4 \lesssim s^{1/2} \lesssim 38.3$ GeV, $|t| = 0.25$ (GeV/c)^2 (Ref. 58) and on the SPS collider ($s^{1/2} = 540$ GeV).[59] These will be discussed in detail in the last Section of the present review.

Finally, experiments on the Batavia accelerator demonstrated an important property of the inclusive cross section $d^2\sigma/dt\,dM_X^2$ as a function of the transferred momentum $|t|$ for fixed high values of M_X^2, namely, a correlation between the slope parameter of DD and the mass of the excited system for large values of M_X^2. As in the case of exclusive of DD processes, the slope parameter is large for $M_X^2 \simeq 1.9$ GeV^2 for which $b \simeq 24$ (GeV/c)$^{-2}$, and then decreases with increasing M_X^2. It is equal to 6 (GeV/c)$^{-2}$ for $M_X^2 \gtrsim 5$ GeV^2, and thereafter is practically independent of mass.[7,15] This behavior of the slope parameter of inelastic proton DD at

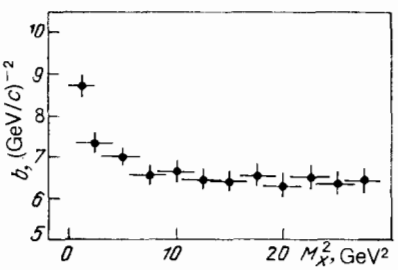

FIG. 15. Slope parameter of the differential cross section for the process pp→Xp as a function of the mass of the excited system.[58]

high energies was subsequently confirmed by experiments performed at CERN on ISR[58] (Fig. 15).

3.2. Impact parameter representation

The impact parameter representation for the elastic scattering amplitude of hadrons [11,12,20,21,60-64] gives a simple and clear picture of high-energy scattering, in which the geometric properties of hadronic interactions are clearly exhibited. It is given by the expression for the elastic scattering amplitude $T(s, t)$ in terms of the profile function $\Gamma(s, b)$, obtained by means of the Fourier-Bessel transformation:

$$T(s, t) = i \int_0^\infty \Gamma(s, b) J_0(b(-t)^{1/2}) b \, db. \tag{3.4}$$

The profile function is useful in writing down the s-channel unitarity condition that expresses the imaginary part of the elastic scattering amplitude, i.e., $\mathrm{Re}\Gamma(s, b)$ in terms of the elastic and inelastic contributions of intermediate states (Refs. 3 and 65):

$$2\mathrm{Re}\,\Gamma(s, b) = |\Gamma(s, b)|^2 + G_{\mathrm{in}}(s, b), \tag{3.5}$$

where $G_{\mathrm{in}}(s, b)$ is the inelastic overlap function[66] that describes absorption into inelastic channels. In the impact parameter representation (3.5), the unitarity expression emphasizes the absorptive nature of diffraction scattering. Actually, if we suppose (in agreement with experiment) that the function $\Gamma(s, b)$ is real, i.e., $T(s, t)$ is purely imaginary, then (3.5) can be solved for $\mathrm{Re}\Gamma(s, t)$:

$$\mathrm{Re}\,\Gamma(s, b) = 1 - (1 - G_{\mathrm{in}}(s, b))^{1/2}. \tag{3.6}$$

Hence it is clear that, if there is no absorption, i.e., $G_{\mathrm{in}}(s, b) = 0$, then there is no elastic scattering either: $\mathrm{Re}\Gamma(s, b) = 0$. This is the mathematical formulation of the physics of the scattering process in which diffraction produces an absorption "shadow" due to the presence of open inelastic channels.[11,12]

In the impact parameter representation, the unitarity condition (3.5), also enables us to give a simple interpretation of the well-known Pumplin relation[67] for total cross sections at a given impact parameter, if we start with the Good-Walker picture (see above).[2] Actually, if for a given impact parameter the bare states $|\chi_k\rangle$ are the eigenstates of the T-matrix, which is assumed to be purely imaginary, i.e.,

$$\mathrm{Im}\,T\,|\,\chi_k\rangle = \tau_k\,|\,\chi_k\rangle, \tag{3.7}$$

then the matrix element of the diffractive transition between physical states has the form ($\alpha_k = U_{1k}$)[2,53,68,69]

$$\langle C\,|\,\mathrm{Im}\,T\,|\,A\rangle = \sum_k c_k^* a_k \tau_k. \tag{3.8}$$

In this approach, the total cross section for given b can be related to the average of the amplitudes $\tau_k(b)$, and the total DD cross section σ_{DD} can be related to their variance (Refs. 12, 53, 68, and 69):

$$\begin{aligned}\sigma_{\mathrm{tot}}(b) &\equiv \frac{d\sigma_{\mathrm{tot}}(b)}{db^2} = 2\mathrm{Re}\,\Gamma(b) = 2\langle C\,|\,\mathrm{Im}\,T(b)\,|\,C\rangle \\ &= 2\sum_k \tau_k(b)\,|\,c_k\,|^2 = 2\langle\tau(b)\rangle, \\ \sigma_{\mathrm{DD}}(b) &= \sum_k |\langle\chi_k\,|\,\mathrm{Im}\,T(b)\,|\,C\rangle|^2 - \sigma_{\mathrm{el}}(b) = \langle\tau^2(b)\rangle - \langle\tau(b)\rangle^2.\end{aligned} \tag{3.9}$$

Since

$$0 \leqslant \tau_k(b) \leqslant 1, \tag{3.10}$$

where the equality sign corresponds to total absorption or total transparency, we have

$$|\,\tau_k(b)\,|^2 \leqslant \tau_k(b). \tag{3.11}$$

From (3.9) we then obtain the restriction on the DD cross section[12,67]

$$\sigma_{\mathrm{DD}}(b) \leqslant \frac{1}{2}\sigma_{\mathrm{tot}}(b) - \sigma_{\mathrm{el}}(b), \tag{3.12}$$

which can be used to analyze experimental data when $\sigma_{\mathrm{tot}}(b)$ and $\sigma_{el}(b)$ are known. Elastic pp scattering data at the ISR energies have been used[7,17] in this way to show that $\sigma_{\mathrm{DD}}(b)$ has a peripheral profile with a maximum at $b = R \simeq 0.7$ fm. This means that, in complete agreement with the Pomeranchuk-Feĭnberg idea,[1] inelastic diffraction is due to the region $b \simeq R$ (scattering by a ring), in contrast to elastic diffraction that arises from interactions throughout the range of b (scattering by a disk).

In precisely the same way, condition (3.5) enables us to determine $G_{\mathrm{in}}(s, b)$ directly from experimental data. Actually, if we know the real and imaginary parts of the elastic scattering amplitude $T(s, t)$, given by (3.4), we can use the inverse Fourier-Bessel transformation

$$\Gamma(s, b) = -i \int_0^\infty (-t)^{1/2}\,d(-t)^{1/2}\,T(s, t)\,J_0(b(-t)^{1/2}) \tag{3.13}$$

to determine $\mathrm{Re}\Gamma(s, b)$ and $\mathrm{Im}\Gamma(s, b)$ and then use (3.5) to obtain $G_{\mathrm{in}}(b)$. This type of analysis of experimental data has frequently been carried out[11,12,62,65,71,72] at the ISR and SPS collider energies. Here we shall consider the results of an analysis reported in a recent paper[72] in which the profile function $\Gamma(b)$ and the inelastic overlap function $G_{\mathrm{in}}(b)$ were determined from experimental data $\bar{\mathrm{p}}\mathrm{p}$ scattering at $p_{\mathrm{L}} = 30$ and 50 GeV/c ($s^{1/2} = 7.6$ and 9.8 GeV and $s^{1/2} = 53$ and 546 GeV).[7)]

It was found that the function $G_{\mathrm{in}}(b)$ had an almost Gaussian form ($\sim\exp(-Bb^2)$): for small b it is slightly higher than the Gaussian distribution, and for large b it was somewhat lower. For $s^{1/2} = 53$ and 546 GeV, $G_{\mathrm{in}}(b)$ was again above the Gaussian function for small b, and the difference was greater at the SPS energies. When $s^{1/2} = 53$ GeV, $G_{\mathrm{in}}(b)$ had a characteristic "tail" for $b \gtrsim 2$ fm, which lay substantially higher than the Gaussian distribution. This phenomenon is due to the change in the slope parameter of the differential cross section $d\sigma/dt$ for small $|t|$, and was found earlier on the ISR[65] in the inelastic overlap function for the pp interaction.

The function $G_{in}(b)$ was described in Ref. 72 for four values of the energy by the expression

$$G_{\mathrm{in}}(b) = C_1 e^{-B_1 b^2} + C_2 b^\nu e^{-B_2 b^2}. \tag{3.14}$$

where the second term has the peripheral profile and describes DD edge effects. This form of $G_{\mathrm{in}}(b)$ was proposed in Refs. 62 and 71 with $\gamma = 2$. It follows from Ref. 72 that (3.14) with $\gamma = 2$ provides a good description of $G_{\mathrm{in}}(b)$, but only for $p_{\mathrm{L}} = 50$ GeV/c. The second term then has a peak at

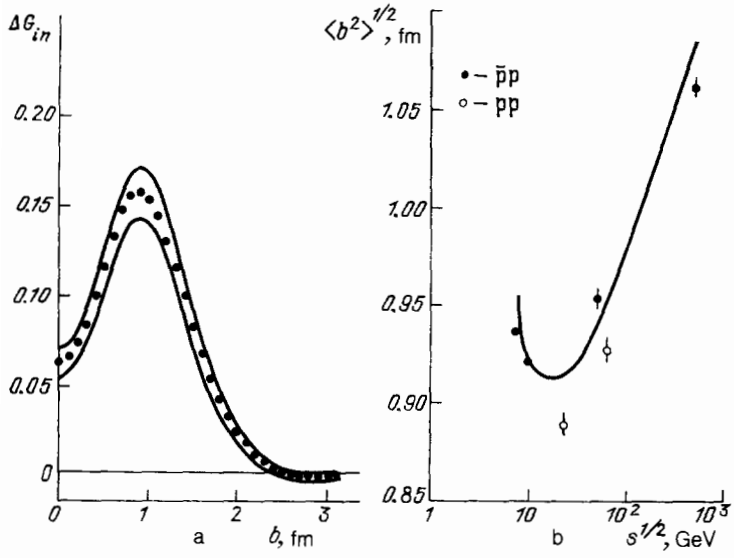

FIG. 16. a—Energy dependence of the function $G_{in}(b)$ for the $\bar{p}p$ interaction with $s^{1/2} = 53$ and 546 GeV.[72] Solid curves show the corridor of systematic uncertainties; b—root mean square range of the $\bar{p}p$ and pp interactions in the impact parameter representation as a function of s (Ref. 65 and 72); solid curve—range of the inelastic interaction in the black disk model: $\sigma \sim \sigma_{in}^{1/2}$.

$b = 0.7$ fm for which its contribution to $G_{in}(b)$ amounts to about 10%.

We note that, since $\Gamma(b = 0) < 1$ for all four values of the energy, there is a nonzero probability that the nucleons will pass through one another without interaction.

The energy dependence of $G_{in}(b)$ was also analyzed in Ref. 72. Figure 16 shows the change $\Delta G_{in}(b)$ in this function between $s^{1/2} = 53$ and $s^{1/2} = 546$ GeV. As can be seen, there is a rapid peripheral increase in the overlap function $G_{in}(b)$ at $b = 0.9$ fm. In addition, there is a relatively large rise (by about 0.06) in the central region ($b = 0$). This is in agreement with the result reported earlier in Ref. 71.

If we know the overlap function, we can determine the mean square radius for inelastic interaction in the impact parameter representation for pp and $\bar{p}p$ collisions. By definition[65]

$$\langle b^2 \rangle^{1/2} = \left[\int_0^{b_{max}} b^2 G_{in}(b)\, b\, db \left(\int_0^{b_{max}} G_{in}(b)\, b\, db \right)^{-1} \right]^{1/2}, \tag{3.15}$$

where b_{max} is determined by the condition

$$G_{in}(s, b_{max}) = 0.085 G_{in}(s, 0). \tag{3.16}$$

Figure 16b shows the results obtained[72] for $\langle b^2 \rangle^{1/2}$ as a function of $s^{1/2}$, together with the results[65] on the pp interaction. It is clear that the mean square radius for the inelastic $\bar{p}p$ interaction increases by about 11% in the range between $s^{1/2} = 53$ and 546 GeV. The pp interaction range[65] at the ISR energies is less than the $\bar{p}p$ range, but it appears to grow more rapidly.

We also note that several other interesting conclusions about the character of the geometric picture of hadronic interactions at high energies follow from the analysis reported in Ref. 72. In particular, the considerable increase (by $\sim 27\%$) in the ratio σ_{el}/σ_{tot} at $s^{1/2} = 53$–546 GeV and the behavior of the inelastic overlap function, do not agree with the predictions of models relying on geometric scaling[73] and the factorized eikonal,[74] which satisfactorily describe experimental results at lower energies.

We emphasize once again that the substantial increase (by $\sim 33\%$) in the inelastic $\bar{p}p$ cross section between the ISR and SPS energies is due to the considerable increase in peripheral absorption (for $b \simeq 0.9$ fm) and a smaller, but still appreciable, increase in absorption in the central region ($b = 0$).

3.3. Reggeon phenomenology and duality

The above impact-parameter representation and the Good-Walker formalism are both based on the s-channel analysis of hadronic interaction processes. In the alternative t-channel approach, which emphasizes the exchange character of hadronic interactions, particle scattering at high energies is described by the Regge model that takes into account the properties of the scattering amplitude in the complex plane of the angular momentum.[26,27,75–77] The model with the triple-reggeon interaction is the most highly developed in relation to DD for high M_x.

The appearance of triple-reggeon vertices in calculations of DD cross section is illustrated in Figs. 17a–c. It is assumed that, when $sM_X^{-2} \gg 1$, the amplitude for the process shown in Fig. 17d can be described by the sum of contribu-

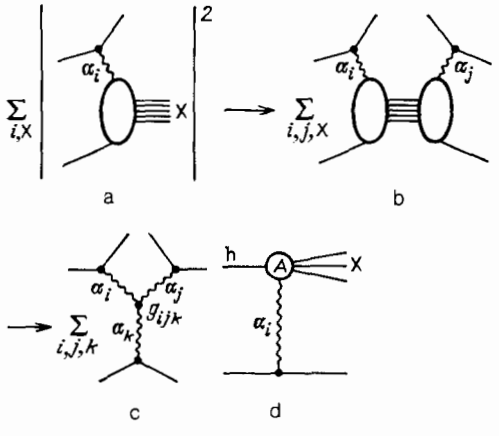

FIG. 17. Inclusive cross section in the triple-reggeon formalism (a–c) and the dissociation amplitude in the Regge model (d).

tions due to the Regge poles

$$T(s,\ t,\ M_X^2) = \sum_i \beta_i(t)\,\xi_i(t)\,A(h+\alpha_i \to X)\left(\frac{s}{M_X^2}\right)^{\alpha_i(t)}, \tag{3.17}$$

where $\beta_i(t)$ is the hadron-reggeon vertex, $\xi_i(t)$ is the signature factor, and the quantity $A(h+\alpha_i \to X)$ can be looked upon as the amplitude for the transition of the hadron h and reggeon α_i to the hadronic state X. Squaring and summing over all the possible states of the system X, we obtain the inclusive cross section

$$\frac{d^2\sigma}{dt\,dM_X^2} = \frac{1}{16\pi s^2}\sum_{i,\,j,\,X}\beta_i\beta_j\xi_i\xi_j^* A(h+\alpha_i \to X) \times A^*(h+\alpha_j \to X)\left(\frac{s}{M_X^2}\right)^{\alpha_i(t)+\alpha_j(t)} \tag{3.18}$$

Let us first consider the diagonal terms ($i=j$) and sum over the states X with fixed M_X^2:

$$\sum_X |A(h+\alpha_i \to X)|^2 = M_X^2\sigma_{h\alpha_i}(M_X^2,\ t), \tag{3.19}$$

where $\sigma_{h\alpha_i}(M_X^2, t)$ is the total cross section for the interaction between the ith reggeon and the hadron when the energy in the center of mass system is M_X^2.

The key point in the analysis of DD in terms of the triple-reggeon formalism is the assumption that the collision between the hadron h and reggeon α_i is completely analogous to the collision between two hadrons. In other words, such collisions lead to identical final states. This means that, as in the case of collisions between hadrons, the overlap of these many-particle inelastic channels (see Fig. 17b) involves the exchange of reggeons and the appearance of vertices that couple different reggeons. This means that, when M_X is large enough, the cross section $\sigma_{h\alpha_i}(M_X^2, t)$ can also be expressed in terms of the contributions of the Regge poles:

$$\sigma_{h\alpha_i}(M_X^2,\ t) = \sum_k \beta_k(0)\,\mathrm{Im}\,\xi_k(0)\,g_{ijk}(t)\,(M_X^2)^{\alpha_k(0)-1}, \tag{3.20}$$

where $g_{ijk}(t)$ is the triple-reggeon vertex shown in Fig. 17c. Substituting (3.19) and (3.20) in (3.18), and taking into account the off-diagonal terms, we finally obtain the following expression[8)] for the inclusive cross section[78]:

$$\frac{d^2\sigma}{dt\,dM_X^2} = \sum_{i,\,j,\,k} G_{ijk}(t)\,s^{\alpha_i(t)+\alpha_j(t)-2}\,(M_X^2)^{\alpha_k(0)-\alpha_i(t)-\alpha_j(t)}, \tag{3.21}$$

where

$$G_{ijk}(t) = \frac{1}{16\pi}\beta_i(t)\,\beta_j(t)\,\xi_i(t)\,\xi_j^*(t)\,\mathrm{Im}\,\xi_k(0)\,\beta_k(0)\,g_{ijk}(t). \tag{3.22}$$

The variables x and p_T are often used in addition to the variables M_X^2 and t. When $M_X^2 s^{-1} \ll 1$, we have $x = 2p_\parallel s^{-1/2} \simeq 1 - (M_X^2/s)$ and $t \simeq -p_T^2$. The dependence of the different contributions to the invariant cross section $s\,d^2\sigma/dt\,dM_X^2$ on s, M_X^2, and x is listed in Table I.

It is clear from Table I that, when the only significant contributions for large M_X are those with $k = \mathbb{P}$, the invariant cross section depends on the single variable x, i.e., we have *scaling*. As noted in the above discussion of experimental data, the cross section $s\,d^2\sigma/dt\,dM_X^2$ satisfies this property within the energy region between the ISR and the SPS collider[59] (see below). The contribution of the triple-pomeron interaction leads to

$$\frac{d^2\sigma}{dt\,dM_X^2} = G_{\mathbb{PPP}}(t)\,s^{2\alpha_{\mathbb{P}}(t)-2}\,(M_X^2)^{\alpha_{\mathbb{P}}(0)-2\alpha_{\mathbb{P}}(t)} = G_{\mathbb{PPP}}(t)\,(1-x)^{1-2\alpha_{\mathbb{P}}(t)}, \tag{3.23}$$

which satisfactorily describes the experimental data.

In general, the differential cross section $d^2\sigma/dtM_X^2$ is determined by the six functions $G_{ijk}(t)$ related to the exchange of the pomeron and the vector and tensor states (the latter are usually described by the effective pole R), and also the two pion terms (see, for example, Ref. 79).

The triple-reggeon model provides a simple method of parametrizing the dependence of the cross section (3.21) on M_X^2, s, and t, and is a convenient basis for the phenomenological analysis of experimental data. In general, the expression given by (3.21) contains a large number of free parameters, and this can only be determined by using experimental data for as wide a range of kinematic variables as possible.

Additional restrictions on the triple-reggeon vertices can be obtained by means of the duality hypothesis. This has turned out to be very fruitful in the study of binary reactions. It finds its mathematical expression in the sum rules[80] that relate the behavior of the scattering amplitudes at low and high energies. A natural generalization of the finite energy sum rules to the reggeon-particle scattering amplitudes leads to the following expression[81]:

TABLE I. Dependence of the invariant cross section $s^2 d^2\sigma/dt\,dM_X^2$ on s, M_X^2, and x in the triple-reggeon limit.

triple-reggeon term	energy dependence	dependence on M_X	x-dependence	scaling
$\mathbb{PPP}$	s^0	M_X^{-2}	$(1-x)^{-1}$	Yes
$\mathbb{PPR}$	$s^{-1/2}$	M_X^{-3}	$(1-x)^{-3/2}$	No
$\mathbb{RRP}$	s^0	M_X^0	$(1-x)^0$	Yes
$\mathbb{RRR}$	$s^{-1/2}$	M_X^{-1}	$(1-x)^{-1/2}$	No

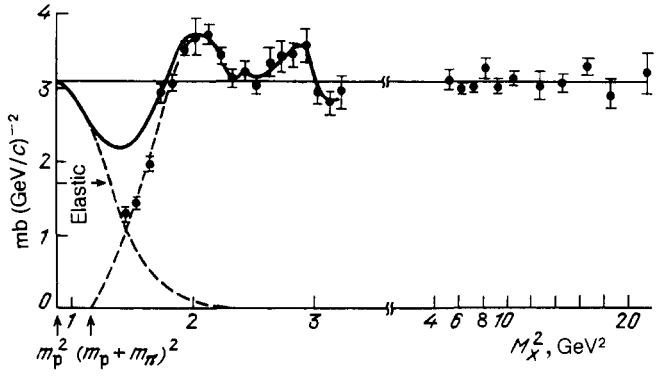

FIG. 18. Verification of the finite mass sum rules for the cross section for the process pd→Xd divided by F_d with $p_L = 275$ GeV/c and $|t| = 0.035$ (GeV/c) (Ref. 8).

$$\int_0^{\nu_0} \nu^n \, d\nu \left[\frac{d^2\sigma}{dt\, dM_X^2}(ab \to cX) + (-1)^{n+1} \frac{d^2\sigma}{dt\, dM_X^2}(cb \to aX) \right] = \sum_{i,j,k} G_{ijk}(t) \frac{s^{\alpha_i(t)+\alpha_j(t)-2} \nu_0^{\alpha_k(0)+n+1-\alpha_i(t)-\alpha_j(t)}}{\alpha_k(0)+n+1-\alpha_i(t)-\alpha_j(t)}, \quad (3.24)$$

which relates the behavior of inclusive cross sections at low M_X to the triple-reggeon asymptotic expressions (3.21). In the above expression, $m = M_X^2 - t - m^2$ is the cross-symmetric variable.

When elastic scattering is taken into account, the sum rule for $m = 1$ can be rewritten in the form

$$|t| \frac{d\sigma_{el}}{dt} + \int_0^{\nu_0} \nu \frac{d^2\sigma}{dt\, d\nu} \, d\nu = \int_0^{\nu_0} \nu \left(\frac{d\sigma}{dt\, d\nu} \right)_{\nu > \nu_0} d\nu, \quad (3.25)$$

in which the right-hand side can be evaluated by a fit to the experimental data in the high-mass region. Figure 18 shows the sum rule (3.25) for the cross section for the process pd→Xd (divided by F_d) for $p_L = 275$ GeV/c and $|t| = 0.035$ (GeV/c)^2 (Ref. 8). It is clear that the extrapolation of the right-hand side of (3.25) to the low-mass region does on average describe the behavior of the left-hand side of (3.25) in this region. If we evaluate the left-hand side of the sum rule using experimental DD data in the region of low M_X, we can use (3.24) as an additional condition for the determination of G_{ijk}. Information on the quantities G_{ijk} is then found to depend significantly on whether or not we can separate in some way the contributions of the $k = \mathbb{P}$ and R terms when we use the finite mass sum rules (3.24). For the usual two-particle hadronic reactions, this separation, based on the two-component duality,[82] turns out to be fully justified. The contribution of the resonances is then related through the finite energy sum rules to the "ordinary" Regge poles R, whereas the background is related to the pomeron $\mathbb{P}$. However, this "normal" two-component duality cannot be generalized to many-particle amplitudes by a direct model-independent method. It is usually assumed that the normal two-component duality obtains for nonpomeron exchange, i.e., for the $R + h \to R + h$ and $R + h \to \mathbb{P} + h$ amplitudes. In the case of the $\mathbb{P} + h \to \mathbb{P} + h$ amplitude, there have been arguments[83] in favor of "abnormal duality" in which resonances in the direct channel "induce" a pomeron in the cross channel. A discussion of all these questions and an analysis of the sum rules (3.24) for estimating the triple-reggeon vertices $G_{ijk}(t)$ can be found in the review literature[15,21] (see also Refs. 77 and 84).

The determination of the triple-reggeon vertices from experimental data on DD spectra is of considerable interest for the theory of strong interactions. The triple-pomeron vertex $G_{ppp}(0)$ is a particularly important characteristic that plays the part of a fundamental constant in the asymptotic Regge field theory.[76] Different regimes arise for $t \to 0$ at asymptotically high energies,[77,85] depending on the behavior of this characteristic.

When $\alpha_p(0) = 1$ and $G_{ppp}(0) \neq 0$, the triple-pomeron contributions to the total cross section, obtained by integrating (3.23), is

$$\sigma_{ppp} \approx \frac{\pi G_{ppp}(0)}{2\alpha_p'(0)} \ln \ln \frac{s}{M_0^2}. \quad (3.26)$$

where M_0 is the lower limit of the region in which the triple-pomeron asymptotic behavior is important. In this case, we have to face a well-known contradiction because the condition $\alpha_p(0) = 1$ means that the total cross section is constant for $s \to \infty$ and the triple-pomeron contribution (3.26) to the total cross section increases with increasing s. The only escape from this dilemma is to annul the triple-pomeron vertex: $G_{ppp}(0) = 0$[76]. The triple-pomeron contribution to the total cross section then tends to a constant limit, and the differential cross sections for all the inelastic processes must vanish as $t \to 0$, whereas the total cross sections for the interaction of all the particles must be asymptotically equal.[86]

The relatively rapid rise in the total cross sections for hadronic interactions, found on the Serpukhov, Batavia, and CERN accelerators, and in cosmic rays, has also stimulated interest in models with $\alpha_p(0) = 1 + \Delta > 1$.[20] For example, it has been shown[87] that, when $\Delta = \Delta_c$, where $\Delta_c = \eta \ln \eta^{-1}$ ["critical pomeron"; $\eta = g_{ppp}^2(0)/32\pi\alpha_p'(0)$], there is a self-consistent solution that satisfies both the t-channel and s-channel unitarity and for which the physical pomeron has $\bar{\alpha}_p(0) = 1$. However, existing estimates of the triple-pomeron vertex, obtained from analyses of DD spectra, suggest a small value of $g_{ppp}(0)$ and, consequently, of Δ_c ($\sim 10^{-2}$), and do not describe the experimentally established increase in the cross sections.[20]

In this context, the most interesting models are those with[88-91] $\Delta > \Delta_c$. In these models ("supercritical pomeron"), the contribution of the pomeron to the total cross section increases as s^Δ at the corresponding energies ($\Delta \ln s < 1$). However, at ultrahigh energies, for which $\Delta \ln s \gg 1$, the total cross section reaches the Froissart state: $\sigma_{tot} \sim \ln^2 s$. This occurs because of the restitution of unitarity during the summing of the alternating-sign series, whose terms represent the contributions of the branches. The effective singularity ("froissaron") in the t-channel, which corresponds to this behavior, shifts toward $j = 1$ for $t = 0$, and is a pair of complex-conjugate branch points. The physical picture of the interaction in the supercritical pomeron theory corresponds for $\ln s \to \infty$ to scattering by a "grey disk" whose radius increases as $\ln s$. In this limit, the cross section for diffraction processes, $\sigma_0 = \sigma_{el} + \sigma_{DD}$, tends to $\frac{1}{2}\sigma_{tot}$ (Ref.

92). Thus, the scattering picture that arises in the framework of the Regge field theory is very close to geometric model of diffraction scattering. It must be remembered, however, that the above regime begins at energies that are practically unattainable ($\Delta \ln s \gg 1$).

The true situation can be much more complicated. In particular, absorptive corrections which, as we have seen, produce a strong modification of the DD amplitude in the low-mass region, may become significant in the triple-reggeon region. Early attempts to take these corrections into account[93] showed that absorption in the triple-pomeron region is sensitive to the slope parameter corresponding to the k th pomeron in the triple-reggeon vertex (see Fig. 17c), and significantly reduces the differential cross section $d^2\sigma dt\, dM_X^2$.

In the supercritical pomeron model, corrections for many-pomeron interactions increase with increasing energy and, as was shown quite recently,[94] they may be considerable even at the energies used in the SPS collider. According to Ref. 94, corrections for multiple-pomeron interactions in the pion dominance model for the vertices of this interaction reduce to the inclusion of the exchange of two and three successively interacting froissarons and to absorption corrections to triple-froissaron exchange. Inclusion of the last corrections substantially reduces the quasi-eikonal for small values of the impact parameter, but their contribution to the total cross section for the NN interaction is less than 3% at the SPS collider energy. The method of allowing for multiple-pomeron corrections developed in Ref. 94 can be successfully used to estimate the total cross section for nucleon DD. At the SPS collider energies, the theoretical value $\sigma_{DD}^{theor} = 9$ mb turns out to be close to the experimental result ($\sigma_{DD}^{exp} = 8.1 \pm 0.8$) mb.[59]

To conclude this Section, we recall the quark-reggeon model of the diffractive excitation of high-mass states,[51] which is a development of the quark model[46] of DD, examined in Section 2. As in the description of the region of low M_X, it is assumed that the pomeron interacts with a dressed quark (in its initial state, the quark lies outside the mass surface) and transfers momentum to it. High-mass states appear as a result of the relative motion that the quarks acquire as a result of scattering. Hadronization of quarks in the final state can also be described in terms of the Regge model. In this approach, all the unknown triple-reggeon vertices can be expressed in terms of parameters determined from the elastic scattering of hadrons and one normalized constant associated with non-mass effects and absorption corrections. The triple-reggeon vertices found in this way give a good description of experimental data on nucleon DD in the region of small $|t|$.

4. FURTHER STUDIES OF THE PROPERTIES OF DIFFRACTIVELY EXCITED SYSTEMS

Diffraction processes continue to be investigated. New interesting results on exclusive DD processes have been obtained in ISR experiments, and measurements of the cross section for the inclusive diffractive excitation of nucleons have been performed on the SPS collider at the highest accelerator energies currently available.

The particular features of the new exclusive experiments include their high statistical precision, coverage of channels that were not previously investigated, and exploration of the mass region well above the threshold. These experiments have concentrated attention on the parton structure of the excited system and on the properties of the diffractive interaction such as direct coupling between the pomeron and the constituents, its similarity to the photon or hadron, and the point character and the coherence of the interaction.[25]

Effects that directly reflect the parton structure of the dissociating particle have been discovered in the course of detailed experimental studies of exclusive channels in the region of "intermediate" masses ($M_X \lesssim 5$) GeV. Experimental results on the following exclusive processes are particularly interesting:

$$pp \to (\Lambda^0 \varphi^0 K^+) p, \tag{4.1}$$

$$pp \to (\Lambda^0 \bar{\Lambda}^0 p) p, \tag{4.2}$$

They were obtained in the R608 experiment on the ISR.[95] A particular feature of these two processes is that the excited system contains one particle that does not have even one valence quark in common with the incident proton (ϕ^0 and $\bar{\Lambda}^0$ particles). The mass distribution of the system created in processes (4.1) and (4.2) does not exhibit a well-defined resonance structure (see Fig. 19). The mass spectrum of the two-particle states does not have well-defined resonance peaks either. This means that the final states in (4.1) and (4.2) are not the decay products of some excited, high-mass baryon. Moreover, these distributions represent the diffraction dynamics in processes (4.1) and (4.2).

All systems, except those that do not contain the valence quarks of the proton, i.e., ϕ^0 and $\bar{\Lambda}^0$, are found to give rise to forward or backward peaks with respect to the Gottfried-Jackson angle (Fig. 20). At the same time, the angular distributions of the ϕ^0 and $\bar{\Lambda}^0$ particles are almost isotropic;

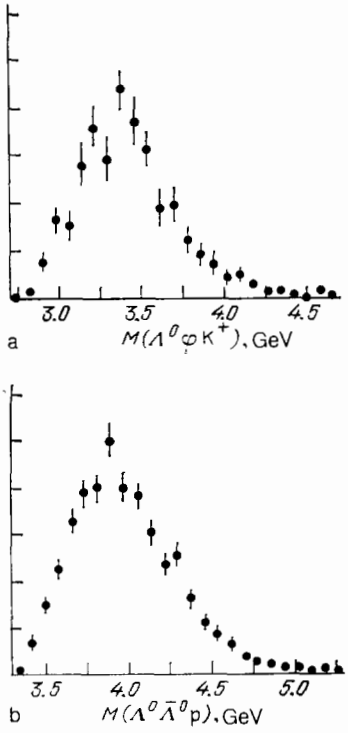

FIG. 19. Distributions over the masses of the $(\Lambda^0\phi^0K^+)$ and $(\Lambda^0\bar{\Lambda}^0p)$ systems in proton DD processes.[95]

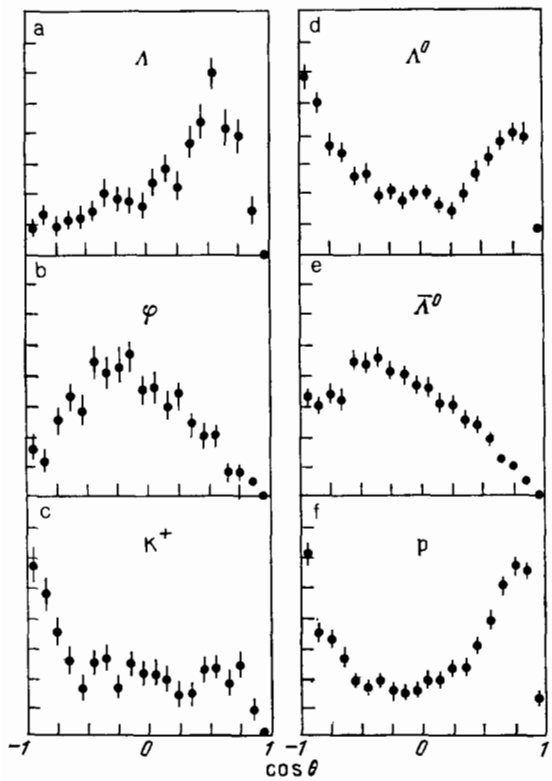

FIG. 20. Distributions over the cosine of the Gottfried-Jackson angle for individual particles from diffractively excited ($\Lambda^0\phi^0K^+$) and ($\Lambda^0\bar{\Lambda}^0p$) systems.[95]

at any rate, they are very different from the angular distributions of the neighboring particles in (4.1) and (4.2). The angular distribution peaks of Fig. 20 are directly correlated. Events in process (4.1) are concentrated in one region, i.e., Λ^0 forward and K^+ backward, whereas in process (4.2) there are two regions, namely, Λ^0 forward, p backward, and p forward, Λ^0 backward. It is clear that these correlations arise for particles containing the valence quarks of the incident proton. In both processes, the Λ^0 particle traveling forward contains the diquark (ud) consisting of the valence quarks of the proton, whereas the backward-traveling K^+ or proton contain the second valence u quark. These properties can be understood with the aid of the quark diagrams of Figs. 21a and b, which predict a forward peak for the Λ^0 particle in

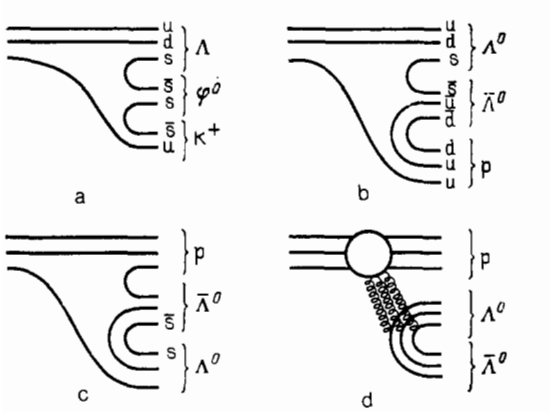

FIG. 21. Quark diagrams for proton DD in ($\Lambda^0\phi^0K^+$), ($\Lambda^0\bar{\Lambda}^0p$), and ($p\Lambda^0\bar{\Lambda}^0$).

processes (4.1) and (4.2), and suggest that the pomeron interacts with an individual u quark from the incident proton.[9] The quark diagrams of Fig. 21c and d predict forward peaks for the proton (Fig. 20d). Figure 21c predicts a peak due to the forward traveling diquark, whereas the u and d quarks are scattered in the backward direction when they interact with the pomeron. As far as the ($\Lambda^0\bar{\Lambda}^0$) system is concerned (isoscalar state), its creation is prevented by the diagram of Fig. 21d which contains the interaction between the pomeron and the gluon component from the gluon sea.[96]

The above quark picture also leads to the central creation and isotropic decay of particles that do not contain the valence quarks of the incident proton [ϕ^0 and $\bar{\Lambda}^0$ in processes (4.1) and (4.2)]. We note further, that all these experimental data are very different from the DD data on $p \to N\pi$ and $p \to 2\pi N$, discussed in Section 2. This is probably due to the fact that the mass range involved in experiment R608 was well removed from the threshold.[97]

The mechanism responsible for the interaction between the pomeron and the constituents of the hadron, including the sea component of the target particle, has also been examined on the basis of huge statistics (eight million events) in the process [98]

$$pp \to (p\pi^+\pi^-\pi^+\pi^-)p. \tag{4.3}$$

The first question to be examined was whether the diffractively created system ($p4\pi$) has isotropic decay properties or a well-defined longitudinal structure. It was found that the momentum of the final proton from the excited system had a tendency to align itself with the momentum of the incident proton, and that this effect was enhanced for higher masses of the diffractively excited system. The pion spectrum exhibits a similar though less well-defined property. We may therefore conclude that studies of both the proton and pion spectra indicate a longitudinal structure of the events.

A more detailed study of these properties was then based on the concept of "sphericity" [99] which measures the quantity p_T^2 relative to the axis of the reconstructed event. It is found by minimizing p_T. Sphericity was not found to be sufficiently sensitive to distinquish the spherically symmetric phase distribution from the longitudinal distribution for the low masses of the diffractively excited systems that were investigated in this experiment. The distribution over the angle between the sphericity axis and the axis of the proton-pomeron collision was found to be more sensitive to the true structure of the events. The latter distribution is shown in Fig. 22 where $\cos\theta = 1$ corresponds to the situation in which the two axes are parallel. The solid and broken curves correspond, respectively, to the longitudinal phase space model and a version of the fireball model. It is clear that the former is better. It satisfactorily describes the mass distribution of both the entire system and the ($p\pi^+$) and ($\pi^+\pi^-$) subsystems. All this enables us to consider[98] that the diffractively created ($p4\pi$) system decays anisotropically and has a longitudinal structure along the direction of the p$\mathbb{P}$ collision. The mechanism in which, after collision, the p$\mathbb{P}$ system recombines, becomes thermalized, and then emits particles randomly and isotropically, is thus incompatible with experimental data. It is important to note that this had been known since the mid 1970s when it was first demonstrated by measurements of the rapidity distributions of particles

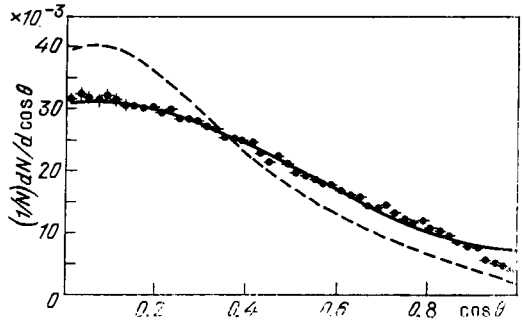

FIG. 22. Distributions over the cosine of the angle between the sphericity axis and the proton-pomeron collision axis for DD to the system (p4π) in the mass range $3 < M_X < 4$ GeV (Ref. 98).

from a diffractively produced beam on the ISR (a detailed discussion can be found, for example, in Ref. 20). Analogous data were obtained on the SPS collider.[59]

The parton structure of the pIP interaction was also revealed by the very unusual properties discovered in the exclusive diffractive production of the D-meson[100]:

$$pp \to \{D(1285)\,p\}\,p. \qquad (4.4)$$

The mass distribution of the forward-emitted system (Dp) has the usual sharp peak for $x \to 1$, typical for all diffraction processes and reflecting the quasi-two-particle nature of the reaction. The unusual properties of process (4.4) are as follows: (1) the mass spectrum of the Dp system does not have a resonance-type structure, (2) the process $p \to pD\pi^0$ is suppressed, (3) the D(1285)-meson in (4.4) is created preferentially for small values of x, and the proton distribution has a sharp forward peak despite the fact that $M_D > m_p$, and (4) studies of the $D(1285) \to \delta^+\pi^-$ decay show that the D-meson is created in a state with a particular helicity ($\lambda_D = \pm 1$). None of these properties can be explained in terms of cluster mechanisms. We note that the suppression of the isovector states ($p \to pD\pi^0$) indicates that the pomeron interacts not with the valence quark but, more likely, with the ($q\bar{q}$) pairs or gluons in the sea.

We have already noted that one of the clearest confirmations of the diffractive dissociation of hadrons, predicted by Pomeranchuk and Feĭnberg, was the experimental discovery of diffractive excitation of hadrons to high-mass states. Since the magnitude of the excited mass M_X is limited only by the coherent nature of the process $[M_X^2 \lesssim s(2mR)^{-1}]$, where $R \sim 1$ fm, the advent of new accelerators, producing higher energies, necessarily leads to an expansion of the range accessible to excitation. There are no fundamental restrictions on the mass of the excited system as the energy of the colliding particles increases.

This is confirmed by the new stage in the experimental investigation of DD phenomena, made possible by the commissioning, at the end of 1981, of the SPS collider at CERN ($s^{1/2} = 546$ GeV), which has meant that diffractive excitation of states with masses in excess of 100 GeV can now be investigated. Let us briefly consider the experimental DD results obtained on the UA4 installation.[59]

Figure 23a shows the invariant differential cross section $(s/\pi)d^2\sigma/dt\,dM_X^2$) for the process $\bar{p}p \to \bar{p}X$ as a function of the variable $M_X^2 s^{-1} \simeq 1 - x$ for fixed values of $|t|$. The experimental data revealed the presence of a quasielastic peak for $M_X^2 s^{-1} \leqslant 0.03$ due to the diffractive creation of high-mass states. The results obtained on the SPS for $M_X^2 s^{-1} \geqslant 0.01$ and $s^{1/2} = 540$ GeV agree, to within systematic uncertainties ($\pm 10\%$) in the absolute normalization, with the invariant cross sections for pp interactions at the ISR energies and the same values of t (Refs. 5, 58, and 101), i.e., they exhibit scaling behavior: they do not depend on s for fixed values of $M_X^2 s^{-1}$ and t (Figs. 23b and c).

Figure 24 shows the cross section $d^2\sigma/dt\,dM_X^2$ for $t = -0.55$ (GeV/c)^2 and $0.1 \leqslant M_X^2/s \leqslant 0.04$ as a function of M_X^2, together with the data obtained on the ISR for the same value of t (Refs. 5, 58, and 101) and the same range of $M_X^2 s^{-1}$. The cross section measured on the SPS is smaller by three orders of magnitude than that obtained on the ISR, and its M_X^2 dependence is described by the same M_X^{-2} relationship that was found earlier at FNAL and on the ISR.

The energy dependence of the total DD cross section is a very important characteristic of diffraction processes.[10] It was found a few years ago in ISR experiments[101] as a result of measurements of the differential cross section $d^2\sigma/dt\,dM_X^2$, followed by integration with respect to t and M_X^2 up to $M_X^2/s \leqslant 0.05$. The total DD cross section σ_{DD} at these energies

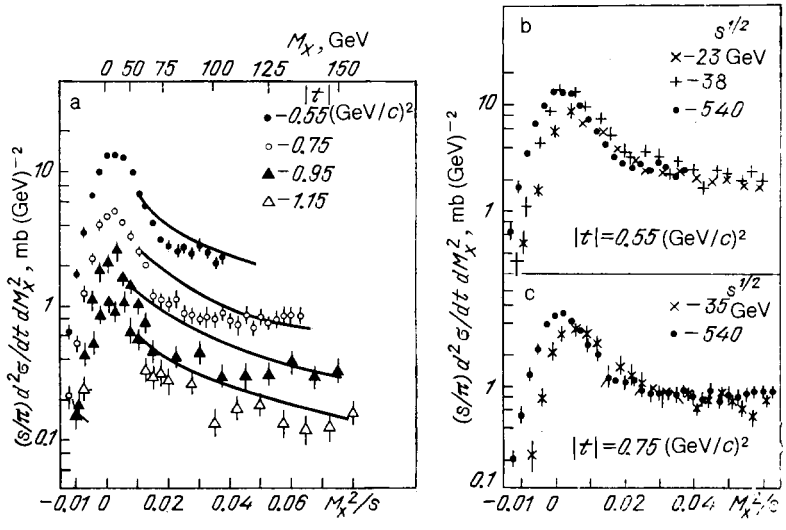

FIG. 23. a—Differential cross section for the process $\bar{p}p \to \bar{p}X$ as a function of $M_X^2 s^{-1}$ for $s^{1/2} = 540$ GeV and different values[59] of $|t|$; theoretical curves from Ref. 105; b, c—differential cross section for the $\bar{p}p$-interaction for different values of s^{-1} and two values of $|t|$ (Ref. 59).

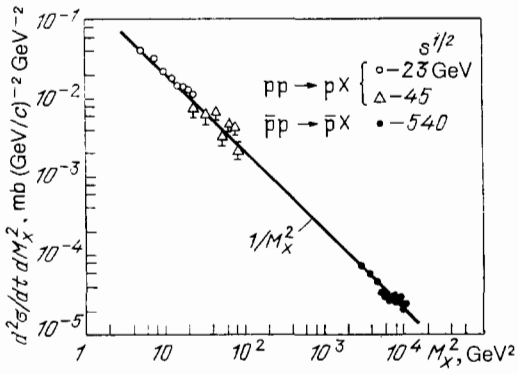

FIG. 24. Differential cross sections for the processes $pp \to pX$ and $\bar{p}p \to \bar{p}X$ as functions of M_X^2 for $|t| = 0.05$ (GeV/c)^2 (Ref. 59).

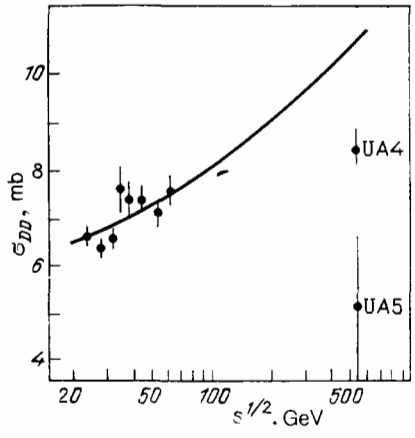

FIG. 25. Total cross section for single DD as a function of energy.[59] The solid curve corresponds to $\sigma_{DD} \sim 0.17\,\sigma_{tot}$.

was found to be comparable with the elastic cross section ($\sigma_{DD}/\sigma_{el} \simeq 1$, $\sigma_{DD}/\sigma_{tot} \simeq 0.17$), and had roughly the same energy dependence as σ_{tot} and σ_{el}. These data are shown in Fig. 25 together with an extrapolation of the relation $\sigma_{DD} = 0.17\sigma_{tot}$ and the preliminary results obtained with the UA4 and UA5 installations on the SPS collider.[59] The latter results indicate a slow increase in σ_{DD} with energy and a smaller contribution of DD to the total cross section: at the SPS collider energies, $\sigma_{DD}/\sigma_{tot} \simeq 0.13$ and $\sigma_{DD}/\sigma_{el} \simeq 0.6$, i.e., the reduction is even greater than at the ISR energies. This behavior is not unexpected within the framework of the Pomeranchuk-Feĭnberg description[1] and corresponds to the geometric picture in which inelastic diffractive scattering occurs on the periphery of the hadron and, consequently, $\sigma_{DD} \sim R$. The increase in R with energy must therefore produce an increase of the form $\sigma_{tot} \sim R^2$ that is faster than the increase in the cross section for inelastic diffraction. Moreover, it must also be remembered that the same Pomeranchuk-Feĭnberg picture provides for a possible increase in the DD cross section due to the creation of particle beams with $M_X \sim s$. Realistic models of diffraction dissociation usually predict a more rapid increase in σ_{DD} (see, for example, Ref. 94) than is indicated by the SPS collider data.[59] In view of the considerable uncertainties in these experimental data, it is at present difficult to draw a definite conclusion with regard to the energy dependence of the DD cross section in this energy range. The acquisition of more accurate data is an important task for future experiments.

As noted above, the main question that has interested us in relation to hadron DD in this review has been that of the properties and nature of the diffractively excited system X. If one assumes the factorization of cross sections for DD processes,[11,22] it turns out that the system is the result of the interaction between the incident hadron and the pomeron. It is therefore natural to suppose that the unknown nature of the $h\mathbb{P}$ interaction should manifest itself in the properties of the diffractively created system, and that these properties and the parton structure of the system are related to the structure and nature of the pomeron.

In this connection, we note once again the frequently stated idea[9,102] that the DD process is the preferred mode of excitation (and investigation) of hadronic states that, for one reason or another, are poorly reflected or not reflected at all in other processes. A possible confirmation of this may be the π' and π'' states with pionic quantum numbers, recently discovered in DD processes, which may be looked upon as the radial excitations of the bound ($q\bar{q}$) states of light quarks.[103] The following may be another example. Detailed analysis of the mass spectrum and of the widths of states created diffractively in the excitation of a proton to the πN system under the influence of different hadrons ($h = \pi$, K, p, $\bar{p}$) have indicated that, in addition to the creation of resonance states that are naturally related to ordinary triple-quark configurations of the group $SU(6) \times O(3)$, there is evidence [104] for the excitation of a narrow state with mass $M(\pi N) \simeq 1.34$ GeV that can be interpreted as the creation of the exotic five-quark system ($q^4\bar{q}$). This is used in Ref. 102 as a basis for suggesting that exotic multiquark states can be created in DD processes as a result of the interaction between a pomeron (an object of special nature) and incident hadrons or, more precisely, the creation of narrow exotic resonances in DD is due to the excitation of the hadronic sea component ($q\bar{q}$ pairs and gluons) under the influence of the pomeron.

We have already mentioned an analogous mechanism in our discussion of experimental data on the exclusive excitation of diffraction states in the intermediate mass range $2 < M_X \lesssim 5$ GeV (see Fig. 21d). We recall that we then mentioned two characteristic features that follow from the structure of the events, namely, the interaction of the pomeron with the individual components of the hadron and the decay of the diffractively excited system in a special direction (along the $p\mathbb{P}$ collision momentum).[25]

Both these properties fit into the framework of the model in which the interaction between the pomeron and the individual quarks in the hadron are examined by analogy with the interaction of an isoscalar photon having a positive C-parity.[105] In this model, the nucleon wave function (in elastic hadron scattering, or in an unexcited hadronic vertex) is taken into account by means of the isoscalar Dirac form factors $F_1(t)$ and $F_2(t)$. The isoscalar form factor F_2 that corresponds to the amplitude with reversed nucleon helicity is shown by elastic eN scattering data to be small, so that the model almost automatically allows for one of the main properties of the pomeron, i.e., the fact that its interaction with the nucleon occurs without helicity reversal. The photon-pomeron analogy, which gives a simple expression for the elastic differential scattering cross section in terms of

the pomeron-quark coupling constant β and the form factor $F_1(t)$ is readily generalized to inelastic diffraction. The differential cross section for the excitation of the mass M_X is[105]

$$\frac{d^2\sigma}{dt\, d(M_X^2/s)} = \frac{9\beta^4}{4\pi} F_1^2(t) \left(\frac{M_X^2}{s}\right)^{1-2\alpha_P(t)} \nu\tilde{W}_2, \qquad (4.5)$$

where the function $\nu\tilde{W}_2$ is related to the structure function for the inelastic scattering of leptons with $q^2 = -t$ and $x_B = -t/M_X^2$. If we use the experimental photoproduction data for $\nu\tilde{W}_2$, and the standard dipole form for the proton form factor $F_1(t) = F_1^p(t)$, and if we determine the coupling constant $\beta(t)$ from experimental data on elastic scattering, we find that (4.5) describes experimental DD data without additional free parameters. This description of the invariant differential cross section for processes of the form $\bar{p}p \to \bar{p}X$ at the SPS collider energies[59] is illustrated in Fig. 23a. Naturally, the model leads to a longitudinal structure of events in the final state that is analogous to deep-inelastic scattering with the leading baryon traveling in the direction of the initial proton.[105,106] However, this does not enable us to draw unambiguous conclusions with regard to the mechanism responsible for the interaction between the pomeron and the incident hadron. Experimental studies of the jet structure of DD processes at high masses[106] may well elucidate this mechanism.

However, it is important to note that, despite its simplicity and successful description of experimental data, the model based on the pomeron-photon analogy has given rise to a number of objections. As noted above, in contrast to the photon, the pomeron may exhibit a significant interaction with the gluon component of the hadron,[18,96,102] which is not taken into account in this model. If we suppose that this interaction with gluons is taken into account by the presence of the cloak of dressed quarks, then we lose the connection with deep-inelastic scattering that involves the participation of current quarks with point interaction.

Of course, the greatest difficiency of phenomenological models that involve the pomeron, including the model decribed above, is that such models do not bring us closer to the explanation of the pomeron in terms of quantum chromodynamics (QCD), i.e., a theory claiming a consistent description of strong interactions.

To conclude this Section,[11)] we must consider, if only briefly, the attempts—so far not very numerous—at describing diffraction dissociation and the nature of the pomeron on the basis of QCD.[107]

Calculations of the asymptotic behavior of the amplitudes for $s \to \infty$ in non-Abelian theories such as QCD are based on the summation of ladder diagrams with Reggeized gluons in the t-channel in the leading logarithmic approximations[108] The gluon ladder diagram (the analog of the pomeron) is the principal object in the perturbative reggeon diagram technique of QCD,[109] constructed by analogy with the usual reggeon diagram technique of Gribov.[76] QCD perturbation theory is also used to calculate the (ladder) gluon interactions corresponding to triple-pomeron vertices of the Regge field theory. In contrast to the usual Regge field theory, the triple-pomeron (ladder) vertices of QCD perturbative theory are not annulled even for zero transferred momentum. This means that the strong-coupling variant[76] for which $\sigma_{tot} \sim (\ln s)^\nu$ ($\nu \leqslant 2$) is to be preferred within the framework of perturbative QCD.

In the QCD Born approximation, the elastic cross section for, say, the $\pi\pi$-interaction, and the DD cross section, are determined by the sum of diagrams with two-gluon exchange in the t-channel.[110–112] Calculations have led to the following relation between the DD cross section and the elastic cross section[112]: $\sigma_{DD} = 0.6\sigma_{el}$, which is in good agreement with the latest experimental data obtained on the SPS collider.[59] When diagrams with two-gluon exchange are evaluated in the Born approximation, the dependence of the DD cross section on the mass of the excited system has the form $d\sigma/dM_X^2 \sim M_X^{-4}$. Diagrams corresponding to the triple-pomeron vertex appear in higher-order perturbation theory. These diagrams describe the excitation of massive states with the cross section $d\sigma/dM_X^{-2} \sim M_X^2$, but they only appear in the next order in α_s as compared with the contribution $\sim M_X^{-4}$ (Ref. 107).

We have frequently noted that, even in the original work of Pomeranchuk and Feĭnberg,[1] it was suggested that the DD cross section at high energies was determined by the interaction corresponding to large values of the impact parameter ($b \gtrsim R$), i.e., it was proportional to the area of the edge of the disk: $\sigma_{DD} \sim 2\pi Rd$, where the width of the edge was $d \sim m_\pi^{-1}$. In the case of the Froissart regime (see Section 3.3),[88–91] we have $\sigma_{tot} = 2\pi R^2$, where the interaction radius is $R \simeq \alpha \ln s$. However, detailed examination of the condition for t-channel unitarity at the point $t = 4m_\pi^2$ has shown that the formula $R \simeq \alpha \ln s$ must have added to it a correction[91] of the form $\beta \ln\ln s$. We then have

$$R(s) = a \ln s - \beta \ln\ln s. \qquad (4.6)$$

Perturbative QCD has been used self-consistently to obtain the energy dependence of the interaction range, taking account of the DD processes.[113] This led to the expression given by (4.6) with $\beta = m_\pi^{-1}$. The pion mass determines the width of the edge of the smoothed θ-function:

$$\tilde{\theta}(R-b) \approx \exp[-2m_\pi(b-R)] \quad \text{for} \quad b > R(s). \qquad (4.7)$$

This enables us to suppress the contribution of enhanced graphs, so that the DD cross section contains in this case the additional small term $(\ln M_X^2)^{-3/2}$:

$$\frac{d\sigma_{DD}}{dM_X^2} \sim \frac{2\pi R \cdot d}{M_X^2 (\ln M_X^2)^{3/2}} \sim \frac{\ln s}{M_X^2 (\ln M_X^2)^{3/2}}. \qquad (4.8)$$

The total DD cross section (integrated with respect to M_X^2) is found to be proportional to $\ln s$. It is thus clear that analysis of the DD processes within the framework of perturbative QCD leads to results that are in qualitative agreement with the Pomeranchuk-Feĭnberg picture and with experimental data.

Nevertheless, there is a number of basic open questions that relate to the nature of the pomeron, e.g., the leading singularity near $j = 1$ with vacuum quantum numbers and a range of diffraction eigenstates.

In QCD, the pomeron emerges as a bound state of two reggeized gluons in the t-channel (glueball exchange). The Born approximation (two-gluon exchange)[110–112] then yields a constant cross section that corresponds to a stationary pole at $j = 1$. The concept of the triple-reggeon interaction localized in rapidity space loses its meaning in this approximation.[114] The point is that, in contrast to the usual $\lambda\phi^3$ theory, QCD allows gluon exchange interactions over short

intervals along the rapidity scale. This means that gluons corresponding to pomeron exchange ($k = \mathbb{P}$ in Fig.17c) can interact with different quarks and not merely with quarks corresponding to i,j reggeon exchanges (Fig.17c), but, for example, one of the gluons can interact with a quark in the incident hadron. This diagram then no longer corresponds to the concept of the triple-reggeon vertex.

When higher order diagrams of the QCD perturbation theory are summed, we find that, instead of the fixed singularity, we have a system of Regge poles for $1 < j < 1 + \Delta$ that aggregate towards the right of the $j = 1$ point.[115] For large $|t|(t = -q^2)$, the evaluation of the trajectory of the bare pomeron can be carried out in QCD using the fact that $j - 1 \sim \alpha_s(q^2) \ll 1$. The leading singularity is then found to move for large q^2, resulting in a power-type increase in the total cross section ($\sigma_{\text{tot}} \sim s^{\Delta}$) in the region in which the leading logarithmic approximation is valid. This is in agreement with existing experimental results.[116] However, it still remains unclear how the results of perturbative QCD, obtained for large $|t|$ for which $\alpha_s(q^2) \ll 1$, can be extended to the diffraction region $t \ll 1$ (GeV/c)^2.

As far as diffraction eigenstates in QCD are concerned,[12)] such states have been found only for certain simple models.[117] For example, in the two-gluon approximation of the component quark model, they correspond to states of the incident hadron with particular values of the relative impact parameter ρ of the $q\bar{q}$ pair (for the meson).[119,112] The cancelation of color in the total interaction then means that the eigenstate depends on ρ^2.

The above results illustrate our present level of understanding of DD problems in terms of QCD which, as we have seen, is not at all complete at present.

5. CONCLUSION

During the 35 years that have elapsed since the appearance of the pioneering paper of Pomeranchuk and Feĭnberg on diffraction dissociation,[1] an enormous amount of work has been done on this interesting phenomenon in the hadronic world. Experimental and theoretical studies of the DD process have significantly deepened and enriched our ideas on the mechanism of diffractive generation and the coherent structure of hadrons. Nevertheless, our understanding of diffraction dissociation is still far from complete. The quark-gluon or QCD-motivated picture of the diffractive interaction is still largely phenomenological and, despite the considerable advances that have been made, cannot claim the status of a theory. The reason for this is, above all, that diffraction phenomena in hadron scattering are closely related in the quark-gluon picture to confinement, and the confinement problem remains unsolved in QCD. It is precisely confinement that determines those properties of hadrons that manifest themselves in diffraction processes, namely, the size of hadrons, their quantum numbers, and the properties of phenomena that occur at large distances, i.e., small transferred momenta, to which diffraction phenomena are largely confined.

During the last decade, the center of gravity of research into the physics of hadrons has shifted toward the so-called "hard" processes, i.e., processes accompanied by large momentum transfers. They occur at short distances, and this enables us to investigate more directly the dynamics of the interaction between the constituents of hadrons, i.e., quarks and gluons. To some extent, these processes have turned out to be simpler than the "soft" diffraction processes, since they are less dependent on confinement.

However, if we wish to investigate coherent interactions between component quarks and gluons, held inside the hadron by confinement forces, we unavoidably face once again a return to soft and, above all, elastic and inelastic diffraction processes. This in turn means that studies of diffraction dissociation continue to remain topical, and must be part of experimental programs for accelerators of the next generation.

The authors are deeply indebted to I. M. Dremin, B. Z. Kapeliovich, and M. G.Ryskin for useful discussions and to A. B. Kaidalov and V. A. Nikitin for valuable suggestions and constructive criticisms.

[1)] When we illustrate different properties of DD processes, we shall as a rule use the results from those experimental papers in which these properties were reported for the first time.

[2)] References to experimental papers can be found in the review given in Ref. 21.

[3)] A more detailed discussion of the dependence of the slope parameter b on the mass M_X and the Gottfried-Jackson angle within the framework of the DHD model can be found in Refs. 14, 16, and 39.

[4)] References to literature and a detailed discussion of these questions can be found in the review paper in Ref. 16.

[5)] We recall that the predictions of the additive quark model for the relationships between the total and differential cross sections and the elements of the density matrix for hadronic processes are in good agreement with experiment and, when the quark spin is taken into account, the model provides a reasonable description of the properties of hadronic resonances.

[6)] References to the experimental data shown in Figs. 10 and 11 can be found in the review papers given in Refs. 15 and 25.

[7)] References to the experimental papers used in these calculations can be found in Ref. 72.

[8)] Here and henceforth we omit the scale factor $s_0 = 1$ GeV^2 in the functional dependence on s and M_X^2.

[9)] It is, however, important to note that analogous results can also be obtained in models in which the gluons forming the pomeron interact with all the quarks in the proton. The important point in relation to observed configurations is that the hadron contains a distribution over the momentum fraction x, and it is this distribution that determines the distribution over the mass of the final system after interaction with the pomeron.

[10)] In this context, the total DD cross section is understood to be the total cross section for single DD: $\sigma_{DD} = \sigma_{SD}$.

[11)] The authors are indebted to M.G.Ryskin for very useful discussions on the questions touched upon here.

[12)] A discussion of this problem can also be found in Refs. 2, 3, 12, 53, 69, and 118.

[1] I. Ya. Pomeranchuk and E. L. Feĭnberg, Dokl. Akad. Nauk SSSR **93**, 439 (1953). E. L. Feĭnberg and I. Ya. Pomeranchuk, Suppl. Nuovo Cimento **3**, 652 (1956).
[2] M. L. Good and W. D. Walker, Phys. Rev. **120**, 1857 (1960).
[3] V. Amaldi, M. Jacob, and G. Matthias, Ann. Rev. Nucl. Sci. **26**, 385 (1976).
[4] S. Drell and K. Hiida, Phys. Rev. Lett. 7, 199 (1961); R. Deck, *ibid.* **13**, 169 (1964).
[5] M. G. Albrow *et al.*, Nucl. Phys. B **51**, 388 (1973); **72**, 376 (1974).
[6] V. Bartenev *et al.*, Phys. Lett. B **51**, 299 (1974).
[7] Y. Akimov *et al.*, Phys. Rev. Lett. **35**, 763, 766 (1975); **39**, 1432 (1977); **40**, 1159 (1978) (E).
[8] Y. Akimov *et al.*, Phys. Rev. D **14**, 3148 (1976).
[9] D. R. O. Morrison, Proc. Fifteenth Intern. Conf. on High Energy Physics, Kiev, 1970, Naukova Dumka, Kiev, 1972.
[10] V. A. Nikitin, Fiz. Elem. Chastits At. Yadra **1**, 7 (1970) [Sov. J. Part. Nucl. **1**, 2 (1970)]. I. M. Gramenitskiĭ and Z. Novak, *ibid.* **5**, 63 (1974) [**5**, 25 (1975)] M. G. Shafranova, *ibid.* p. 645 [**5**, 259 (1975)].
[11] F. Zachariazen, Phys. Rep. C **2**, 1 (1971). D. W. G. Leith, Proc. SLAC Summer Institute on Particle Physics: SLAC Report No. 179 **1**, 1 (1974).
[12] H. I. Miettinen, Preprint TH. 1864, CERN, Geneva, 1974; Proc. EPS Intern. Conf. on High Energy Physics, Palermo, 1975, p. 731.

[13]L. A. Ponomarev, Fiz. Elem. Chastits At. Yadra **7**, 186 (1976) [Sov. J. Part. Nucl. **7**, 70 (1976)].
[14]A. B. Kaidalov, Proc. Eighteenth Intern. Conf. on High Energy Physics, Tbilisi, 1976; JINR Dl. 2-10400, Dubna, 1977, p. Al-27; L. A. Ponomarev, *ibid.* Al-24; Yad. Fiz. **27**, 1342 (1978) [Sov. J. Nucl. Phys. **27**, 708 (1978)]; V. A. Lyubimov, Usp. Fiz. Nauk **121**, 193 (1977) [Sov. Phys. Usp. **20**, 97 (1977)].
[15]S. V. Mukhin and V. A. Tsarev, Fiz. Elem. Chastits At. Yadra **8**, 989 (1977) [Sov. J. Part. Nucl. **8**, 403 (1977)].
[16]N. P. Zotov and V. A. Tsarev, *ibid.* **9**, 650 (1978) [**9**, 266 (1978)].
[17]V. A. Tsarev, Proc. 1977 European Conf. on Particle Physics, Budapest, 1977, Vol. 1, p. 83; Proc. Nineteenth Intern. Conf. on High Energy Physics, Tokyo, 1978, p. 639.
[18]V. A. Tsarev, Proc. Fifth Intern. Seminar on High-Energy Physics [in Russian], Joint Institute for Nuclear Research, Dubna, 1978, p. 221.
[19]V. A. Nikitin, Proc. Intern. Conf. on High Energy Physics, Geneva, 1979, Vol. 2, p. 547.
[20]A. B. Kaĭdalov, Phys. Rep. **50**, 157 (1979).
[21]G. Alberi and G. Goggi, *ibid.* **74**, 1 (1981).
[22]K. Goulianos, *ibid.* **101**, 169 (1983).
[23]A. R. White, Preprint FERMILAB-Conf.-82/16-THY, 1982; Preprint ANL-HEP-83-23, 1983; Preprint ANL-HEP-CP-85-104, 1985.
[24]I. A. Kuchin, Diffractive Dissociation [in Russian], Nauka, Alma-Ata, Kaz. SSR, 1984.
[25]Elastic and Diffractive Scattering at the Collider and Beyond, ed. by B. Nicolescu and J. Tran Thanh Van, Editions Frontiéres, Paris, 1985.
[26]H. D. I. Abarbanel, J. B. Bronzan, R. L. Sugar, and A. R. White, Phys. Rep. C. **21**, 119 (1975).
[27]M. Baker and K. A. Ter-Martirosyan, *ibid.* **28**, 1 (1976).
[28]E. W. Anderson *et al.*, Phys. Rev. Lett. **16**, 855 (1966).
[29]I. M. Blair *et al.*, *ibid.* **17**, 789.
[30]E. W. Anderson *et al.*, *ibid.* **25**, 699 (1970).
[31]R. M. Edelstein *et al.*, Phys. Rev. D **5**, 1073 (1972).
[32]J. V. Allaby *et al.*, Nucl. Phys. B **52**, 316 (1973).
[33]H. De Kerret *et al.*, Phys. Lett. B **63**, 477 (1976).
[34]R. Webb *et al.*, *ibid.* **55**. 331 (1975).
[35]J. Biel *et al.*, Phys. Rev. Lett. **36**, 504, 507, 1976; Phys. Lett. B **65**, 291 (1976); Phys. Rev. D **18**, 3079 (1978).
[36]T. Ferbel, Preprint UR-546-COO-3065-124, 1975.
[37]G. Ascoli *et al.*, Phys. Rev. D **7**, 669 (1973); **8**, 3894; **9**, 1963 (1974); Y. M. Antipov *et al.*, Nucl. Phys. B **63**, 141, 153 (1973).
[38]G. Otter *et al.*, *ibid.* **93**, 365 (1975); **106**, 77 (1976). G. W. Brandenburg *et al.*, Phys. Rev. Lett. **36**, 703 (1976).
[39]A. Babaev *et al.*, Nucl. Phys. B **116**, 28 (1976).
[40]V. A. Tsarev, Phys. Rev. D **11**, 1864 (1975).
[41]E. L. Berger, Argonne Report ANL-HEP-PR-75-06, 1975.
[42]H. I. Miettinen and P. Pirila, Phys. Lett. B **40**, 127 (1972).
[43]E. L. Berger and P. Pirila, Phys. Rev. D **12**, 3448 (1975).
[44]E. L. Berger, *ibid.* **11**, 3214; Argonne Report ANL-HEP-PR-75-32, 1975.
[45]P. Söding, Phys. Lett. **19**, 702 (1966).
[46]V. A. Tsarev, Yad. Fiz. **28**, 1054 (1978) [Sov. J. Nucl. Phys. **28**, 541 (1978)].
[47]V. V. Anisovich, E. M. Levin, and M. G. Ryskin, Yad. Fiz. **29**, 1311 (1979) [Sov. J. Nucl. Phys. **29**, 674 (1979)].
[48]E. M. Levin and V. N. Shekhter, Proc. Ninth Winter School [in Russian], Leningrad Institute of Nuclear Physics, 1974, p. 28. V. V. Anisovich, *ibid.* p. 106; G. Altarelli *et al.*, Nucl. Phys. B **69**, 531 (1974).
[49]R. C. Hwa, Phys. Rev. D **22**, 759, 1593 (1980); University of Oregon preprint OITS 206, 1983.
[50]E. M. Levin and L. L. Frankfurt, Usp. Fiz. Nauk **94**, 243 (1968) [Sov. Phys. Usp. **11**, 106 (1968)]. J. J. Kokkedee, *The Quark Models* Benjamin, N. Y., 1969 [Russ. transl., Mir, M., 1971].
[51]S. V. Mukhin and V. A. Tsarev, Yad. Fiz. **30**, 1680 (1979) [Sov. J. Nucl. Phys. **30**, 873 (1979)].
[52]V. M. Braun and Yu. M. Shabelski, LNPI Preprint 682, Leningrad, 1981.
[53]H. I. Miettinen and J. Pumplin, Phys. Rev. D **18**, 1696 (1978).
[54]L. Van Hove and K. Fialkowski, Nucl. Phys. B **107**, 211 (1976).
[55]A. Bialas and A. Czachor, Preprint TP JU-25/77, 1977.
[56]N. P. Zotov and V. A. Tsarev, Kratk. Soobshch. Fiz. No. 3, 28 (1980) [Sov. Phys. Lebedev Inst. Rep. No. 27 (1980)]; N. P. Zotov, V. A. Saleev, and V. A. Tsarev, "Problems in atomic science and technology," General and Atomic Physics [in Russian], TsNIIatomizdat, M., 1983, No. 1(22), p. 85. Preprint FIAN SSSR No. 196 [in Russian], M., 1985.
[57]K. Abe *et al.*, Phys. Rev. Lett. **30**, 766 (1973).
[58]G. Albrow *et al.*, Nucl. Phys. B **108**, 1 (1976).
[59]V. Palladino, Ref. 25, p. 79.
[60]U. Amaldi, Proc. Intern. Conf. on Elementary Particles, Aix-en-Provence, France, 1973; J. Phys. (Paris) **10**, Cl-241 (1973).
[61]A. W. Chao and C. N. Yang, Phys. Rev. D **8**, 2063 (1973).
[62]R. Henzi and P. Valin, Phys. Lett. B **48**, 119 (1974).
[63]F. S. Heney, R. Hong Tuan, and G. L. Kane, Nucl. Phys. B **70**, 445 (1974).
[64]W. Grein, R. Guigas, and P. Kroll, *ibid.* **89**, 93 (1975). N. P. Zotov, S. V. Rusakov, and V. A. Tsarev, Fiz. Elem. Chastits At. Yadra **11**, 1160 (1980) [Sov. J. Part. Nucl. **11**, 462 (1980)].
[65]U. Amaldi and K. R. Schubert, Nucl. Phys. B **166**, 301 (1980).
[66]L. Van Hove, Nuovo Cimento **28**, 798 (1963); Rev. Mod. Phys. **36**, 655 (1964).
[67]J. Pumplin, Phys. Rev. **8**, 2899 (1973).
[68]A. Bialas, W. Czyz, and A. Kotanski, Ann. Phys. (Paris) **73**, 439 (1972).
[69]B. Z. Kopeliovich and L. I. Lapidus, Pis'ma Zh. Eksp. Teor. Fiz. **28**, 664 (1978) [JETP Lett. **28**, 614 (1978)]; *Multiple Production and Limiting Fragmentation of Nuclei* [in Russian], Joint Institute for Nuclear Research, Dubna, 1979, p. 678.
[70]L. Caneshi, P. Crassberger, H. I. Miettinen, and F. S. Henyey, Phys. Lett. B **56**, 359 (1975).
[71]R. Henzi and P. Valin, *ibid.* **132**, 443 (1983).
[72]T. Fearnley, Preprint CERN-EP/85-137, 1985.
[73]J. Dias de Deus, Nucl. Phys. B **59**, 231 (1973); A. J. Buras and J. Dias de Deus, *ibid.* **71**, 481 (1974); J. Dias de Deus and P. Kroll, Acta Phys. Pol. B **9**, 159 (1978); P. Kroll, Z. Phys. C **15**, 67 (1982).
[74]F. Hayot and U. P. Sukhatme, Phys. Rev. D **10**, 2183 (1974); T. T. Chou and C. N. Yang, *ibid* **19**, 3268 (1979). C. Bourrely, J. Soffer, and T. T. Wu, *ibid.* 3249; Nucl. Phys. B **247**, 15 (1984).
[75]T. Regge, Nuovo Cimento **14**, 951 (1959); **18**, 947 (1960); G. F. Chew and S. C. Frautschi, Phys. Rev. Lett. **7**, 394 (1961); Phys. Rev. **126**, 1202 (1962); S. C. Frautschi, M. Gell-Mann, and F. Zachariazen, *ibid.* 2204; V. N. Gribov, Zh. Eksp. Teor. Fiz. **41**, 667, 1962 (1961) [Sov. Phys. JETP **14**, 478 (1962)]; V. N. Gribov and I. Ya. Pomeranchuk, *ibid.* **42**, 1141 (1962) [**15**, 788 (1962)]; **43**, 308 [**16**, 220 (1963)].
[76]V. N. Gribov, *ibid.* **53**, 654 (1967) [**26**, 414 (1968)] V. N. Gribov and A. A. Migdal, Yad. Fiz. **8**, 1002 (1968) [Sov. J. Nucl. Phys. **8**, 583 (1969)]. Zh. Eksp. Teor. Fiz. **55**, 1498 (1968) [Sov. Phys. JETP **28**, 784 (1969)].
[77]P. D. Collins, *An Introduction to Regge Theory and High Energy Physics*, Cambridge University, Cambridge Press (1977) [Russ. transl., Atomizdat, M., 1980].
[78]O. V. Kancheli, Pis'ma Zh. Eksp. Teor. Fiz. **11**, 397 (1970) [JETP Lett. **11**, 267 (1970)]; A. M. Mueller, Phys. Rev. D **2**, 2963 (1970).
[79]V. A. Tsarev, *ibid.* **11**, 1875 (1975).
[80]A. A. Logunov, L. D. Soloviev, and A. N. Tavkhelidze, Phys. Lett. B **24**, 181 (1967) K. Igi and S. Matsuda, Phys. Rev. Lett. **18**, 625 (1967). Y. Liu and S. Okubo, *ibid.* **19**, 190. R. Dolen, D. Horn, and C. Schmid, *ibid.* 402.
[81]J. Kwiecinski, Nuovo Cimento **3**, 619 (1972). M. B. Einhorn, J. E. Ellis, and J. Finkelstein, Phys. Rev. D **5**, 2063 (1972). A. I. Sanda, *ibid.* **6**, 280.
[82]P. G. O. Freund, Phys. Rev. Lett. **20**, 235 (1968). H. Harari, *ibid.* 1395.
[83]M. B. Einhorn, M. B. Green, and M. A. Virasoro, Phys. Lett. B **37**, 292 (1971).
[84]R. D. Field and G. C. Fox, Nucl. Phys. B **80**, 367 (1974). S. Y. Chu, B. R. Desai, B. C. Shen, and R. D. Field, Phys. Rev. D **13**, 2967 (1976).
[85]A. B. Kaĭdalov, Eighth Winter School at Leningrad Institute of Nuclear Physics [in Russian], Leningrad Institute of Nuclear Physics, Academy of Sciences of the USSR, 1973, p. 83.
[86]V. N. Gribov, Yad. Fiz. **17**, 603 (1973) [Sov. J. Nucl. Phys. **17**, 313 (1973)].
[87]A. A. Migdal, A. M. Polyakov, and K. A. Ter-Martirosyan, Phys. Lett. B **48**, 239 (1974); H. D. I. Abarbanel and J. B. Bronzan, *ibid.* 345.
[88]H. Cheng and T. Wu, Phys. Rev. Lett. **24**, 1456 (1970); Phys. Lett. B **44**, 97 (1973).
[89]J. L. Cardy, Nucl. Phys. B **75**, 413 (1974).
[90]D. Amati *et al.*, Phys. Lett. B **56**, 465 (1975); Nucl. Phys. B **101**, 397 (1975); **112**, 107 (1976); **114**, 483.
[91]M. S. Dubovikov and K. A. Ter-Martirosyan, Preprint ITEF-37, M., 1976. B. Z. Kopeliovich and L. I. Lapidus, Zh. Eksp. Teor. Fiz. **71**, 61 (1976) [Sov. Phys. JETP **44**, 31 (1976)]; M. S. Dubovikov *et al.*, Nucl. Phys. B **123**, 147 (1977); M. S. Dubovikov and K. A. Ter-Martirosyan, *ibid.* **124**, 163.
[92]A. B. Kaĭdalov, "Elementary particles," Eleventh School of Physics at ITEF [in Russian], Energoatomizdat, M., 1984, No. 4, p. 3.
[93]A. Capella, J. Kaplan, and J. Tran Thanh Van, Nucl. Phys. B **105**, 333 (1976); V. A. Abramovskiĭ, Pis'ma Zh. Eksp. Teor. Fiz. **23**, 228 (1976) [JETP Lett. **23**, 205 (1976)].
[94]A. B. Kaĭdalov, L. A. Ponomarev, and K. A. Ter-Martirosyan, Preprint ITEP-41, M., 1986.
[95]S. Erhan and J. Alitti, see Ref. 25, p. 121.
[96]P. Chauvat *et al.*, Phys. Lett. B **148**, 382 (1984).

[97]A. Donnachie, see Ref. 25, p. 393.
[98]M. Medinnis, *ibid.* p. 113.
[99]J. D. Bjorken and S. D. Brodsky, Phys. Rev. D **1**, 1416 (1970).
[100]P. E. Schlein, see Ref. 25, p. 107.
[101]J. C. M. Armitage *et al.*, Nucl. Phys. B **194**, 365 (1982).
[102]M. Markytan, T. Hirose, and T. Kobayashi, Preprint KEK 81-9, 1981.
[103]M. A. Anan'ev *et al.*, Preprint OIYaI Rl-81-556, Dubna, 1981.
[104]T. Hirose *et al.*, Nuovo Cimento A **50**, 120 (1979). C. Fukunaga, *ibid.* **58**, 199 (1980).
[105]A. Donnachie and P. V. Landshoff, Phys. Lett. B **123**, 345 (1983); Nucl. Phys. B **231**, 189 (1984); **244**, 322; see Ref. 25, p. 209.
[106]G. Ingelman, *ibid.*, p. 135; G. Ingelman and P. E. Schlein, Phys. Lett. B **152**, 256 (1985).
[107]L. V. Gribov, E. M. Levin, and M. G. Ryskin, Phys. Rep. **100**, 1 (1983).
[108]Ya. Ya. Balitskiĭ, L. N. Lipatov, and V. S. Fadin, Fourteenth Winter School at Leningrad Institute of Nuclear Physics [in Russian], Leningrad Institute of Nuclear Physics, Academy of Sciences of the USSR, 1979, p. 109.
[109]L. V. Gribov, E. M. Levin, and M. G. Ryskin, Yad. Fiz. **35**, 1278 (1982) [Sov. J. Nucl. Phys. **35**, 749 (1982)].
[110]F. E. Low, Phys. Rev. D **12**, 163 (1975). S. Nussinov, Phys. Rev. Lett. **34**, 1286 (1975); Phys. Rev. D. **14**, 246 (1976).
[111]J. F. Gunion and D. E. Soper, *ibid.* **15**, 2617 (1977); Ya. Ya. Balitskiĭ and L. N. Lipatov, Pis'ma Zh. Eksp. Teor. Fiz. **30**, 383 (1979) [JETP Lett. **30**, 355 (1979)].
[112]E. M. Levin and M. G. Ryskin, Yad. Fiz. **34**, 1114 (1981) [Sov. J. Nucl. Phys. **34**, 619 (1981)].
[113]E. M. Levin and M. G. Ryskin, LNPI preprint 370, Leningrad, 1977; M. G. Ryskin, Twelfth All-Union School on Nuclear Interactions at High and Ultrahigh Energies [in Russian], Bakuriani, GSSR, 1987.
[114]B. Z. Kopeliovich and N. A. Russakovich, JINR Preprint E2-86-298, Dubna, 1986.
[115]E. A. Kuraev, L. N. Lipatov, and V. S. Fadin, Zh. Eksp. Teor. Fiz. **72**, 377 (1977) [Sov. Phys. JETP **45**, 199 (1977)]. L. N. Lipatov, *ibid.* **90**, 1536 (1986) [**63**, 904 (1986)].
[116]B. Z. Kopeliovich, Proc. Twentieth Winter School at Leningrad Institute of Nuclear Physics [in Russian], Leningrad Institute of Nuclear Physics, Academy of Sciences of the USSR, 1985, p. 140; B. Z. Kopeliovich and B. G. Zakharov, JINR Preprint E2-86-707, Dubna, 1986.
[117]B. Z. Kopeliovich, N. N. Nikolaev, and I. K. Potashnikova, JINR Preprint E2-86-125, Dubna, 1986.
[118]N. N. Nikolaev, Usp. Fiz. Nauk **134**, 369 (1981) [Sov. Phys. Usp. **24**, 531 (1981)].
[119]A. B. Zamolodchikov, B. Z. Kopeliovich, and L. I. Lapidus, Pis'ma Zh. Eksp. Teor. Fiz. **33**, 612 (1981) [JETP Lett. **33**, 595 (1981)].
[120]G. Bertsch *et al.*, Phys. Rev. Lett. **47**, 297 (1981).

Translated by S. Chomet